

พอลิเมอร์จำรูปร่างชนิดใหม่จากโคพอลิเมอร์ของพอลิเบนซอกซาซินฐานชีวภาพ/อีพอกซีฐานชีวภาพ



นางสาวผกากรอง หอมบุญมา

บทคัดย่อและแฟ้มข้อมูลฉบับเต็มของวิทยานิพนธ์ตั้งแต่ปีการศึกษา 2554 ที่ให้บริการในคลังปัญญาจุฬาฯ (CUIR)
เป็นแฟ้มข้อมูลของนิสิตเจ้าของวิทยานิพนธ์ ที่ส่งผ่านทางบัณฑิตวิทยาลัย

The abstract and full text of theses from the academic year 2011 in Chulalongkorn University Intellectual Repository (CUIR)
are the thesis authors' files submitted through the University Graduate School.

วิทยานิพนธ์นี้เป็นส่วนหนึ่งของการศึกษาตามหลักสูตรปริญญาวิศวกรรมศาสตรมหาบัณฑิต

สาขาวิชาวิศวกรรมเคมี ภาควิชาวิศวกรรมเคมี

คณะวิศวกรรมศาสตร์ จุฬาลงกรณ์มหาวิทยาลัย

ปีการศึกษา 2560

ลิขสิทธิ์ของจุฬาลงกรณ์มหาวิทยาลัย

Novel Shape Memory Polymer from Bio-Based Polybenzoxazine/Bio-
Based Epoxy Copolymers

Miss Phakakrong Hombunma



A Thesis Submitted in Partial Fulfillment of the Requirements
for the Degree of Master of Engineering Program in Chemical Engineering

Department of Chemical Engineering

Faculty of Engineering

Chulalongkorn University

Academic Year 2017

Copyright of Chulalongkorn University

Thesis Title Novel Shape Memory Polymer from Bio-Based
Polybenzoxazine/Bio-Based Epoxy Copolymers
By Miss Phakakrong Hombunma
Field of Study Chemical Engineering
Thesis Advisor Professor Sarawut Rimdusit, Ph.D.

Accepted by the Faculty of Engineering, Chulalongkorn University in Partial
Fulfillment of the Requirements for the Master's Degree

.....Dean of the Faculty of Engineering
(Associate Professor Supot Teachavorasinskun, D.Eng.)

THESIS COMMITTEE

.....Chairman
(Professor Siriporn Damrongsakkul, Ph.D.)

.....Thesis Advisor
(Professor Sarawut Rimdusit, Ph.D.)

.....Examiner
(Paravee Vas-Umnuay, Ph.D.)

.....External Examiner
(Associate Professor Chirakarn Muangnapoh, Dr.Ing.)

จุฬาลงกรณ์มหาวิทยาลัย
CHULALONGKORN UNIVERSITY

5970250221 : MAJOR CHEMICAL ENGINEERING

KEYWORDS: SHAPE MEMORY POLYMER, VANILLIN-FURFURYLAMINE BASED BENZOXAZINE, EUGENOL-FURFURYLAMINE BASED BENZOXAZINE

PHAKAKRONG HOMBUNMA: Novel Shape Memory Polymer from Bio- Based Polybenzoxazine/ Bio- Based Epoxy Copolymers. ADVISOR: PROF. SARAWUT RIMDUSIT, Ph.D., 71 pp.

Shape memory polymers (SMPs) are known as smart polymer materials which can be deformed and fixed in a temporary shape and can recover to its original shape upon an external stimulus such as temperature which is the main stimulus for general SMPs. In this research, a renewable natural resource based on vanillin-furfurylamine benzoxazine (V-fa) and eugenol-furfurylamine benzoxazine (E-fa) are developed to substitute the use of petroleum based polybenzoxazine. The as-synthesized V-fa and E-fa show the degradation temperature at 5% weight loss to be as high as 343 and 310°C and char content to be 66 and 54%, respectively. Effects of epoxidized castor oil (ECO) content at 10-50wt% filled in bio-based polybenzoxazine on thermal, mechanical and shape memory properties of bio-based polybenzoxazine/bio-based epoxy SMPs are thoroughly investigated. The results reveal that with increase in ECO content, storage modulus and glass transition temperature of V-fa/ECO and E-fa/ECO copolymer decreased providing the values of 2.27 GPa to 1.60 GPa and 158°C to 100°C, respectively for V-fa/ECO copolymer and 1.53 GPa to 1.16 GPa and 40°C to -17°C, respectively for E-fa/ECO copolymer. In shape memory properties, the V-fa/ECO SMPs show shape fixity values at a room temperature of 86-94% and the values decrease with increasing ECO content, while the temporary shape at room temperature of the E-fa/ECO SMPs cannot fixed. Additionally, the V-fa/ECO SMPs provided the shape recovery values at $T_g+20^\circ\text{C}$ of 81-96% and the values increase with increasing of ECO content. Furthermore, it was observed that the V-fa/ECO copolymer having 40wt% of V-fa content exhibits good balance properties between shape memory performance and thermomechanical properties and it can be greatly recovered to the original shape for 5 cycles.

Department: Chemical Engineering

Student's Signature

Field of Study: Chemical Engineering

Advisor's Signature

Academic Year: 2017

ACKNOWLEDGEMENTS

The author would like to express my sincerest gratitude and deep appreciation to my advisors, Prof. Dr. Sarawut Rimdusit, for their invaluable guidance and suggestions including constant encourage throughout this study. The author is also grateful to my committee members, who provided constructive and scientific advices for the completion of this thesis. This includes, Prof. Dr. Siriporn Damrongsakkul as the chairman and Dr. Paravee Vas-Umnuay from the Department of Chemical Engineering, Faculty of Engineering, Chulalongkorn University, and Assoc. Prof. Dr. Chirakarn Muangnapoh.

This research has been supported by the Ratchadaphiseksomphot Endowment Fund of Chulalongkorn University, the Institutional Research Grant (The Thailand Research Fund), IRG 5780014, Department of Chemical Engineering, Chulalongkorn University, Contract No.RES_57_411_21_076 and Epoxidized castor oil was supported by Aditya Birla Chemical (Thailand). Additionally, I would like to extend my grateful thanks to all members of Polymer Engineering Laboratory of the Department of Chemical Engineering, Faculty of Engineering, Chulalongkorn University, for their assistance, discussion, and friendly encouragement in solving problems. Finally, my deepest regard to my family and parents, who have always been the source of my unconditional love, understanding, support and encouragement during my studies. Also, every person who deserves thanks for encouragement and support that cannot be listed.

CONTENTS

	Page
THAI ABSTRACT	iv
ENGLISH ABSTRACT	v
ACKNOWLEDGEMENTS	vi
CONTENTS	vii
CHAPTER I INTRODUCTION.....	3
1.1 Overview	3
1.2 Objectives	4
1.3 Scope of the study	4
1.4 Procedure of the study.....	5
CHAPTER II THEORY	6
2.1 Shape Memory Polymers (SMPs).....	6
2.2 Epoxy Resin	20
2.3 Benzoxazine Resin	24
CHAPTER III LITERATURE REVIEW	26
CHAPTER IV EXPERIMENTAL.....	43
4.1 Raw Materials	43
4.2 Resin Preparation.....	43
4.3 Characterization Methods.....	44
CHAPTER V RESULTS AND DISCUSSION	47
5.1 Chemical structure of V-fa and E-fa based benzoxazine monomer	47
5.2. Thermal Stability of Bio-Based Benzoxazine/Bio-Based Epoxy Copolymer	48
5.3 Dynamic Mechanical Properties of Bio-Based Benzoxazine/Bio-Based Epoxy Copolymer.....	51

	Page
5.4 Shape Memory Properties	54
5.5 Repeated fold-deploy cycles	62
CHAPTER VI CONCLUSIONS	63
REFERENCES	66
VITA.....	71



LISTS OF FIGURES

Figure 2.1 Temperature dependency of elasticity modulus of SMP	6
Figure 2.2 Schematic illustrations of (a) Dual-shape memory effect and (b) Triple-shape memory effect.	7
Figure 2.3 Schematic of thermo-mechanical cycle leading to strain recovery for a shape memory polymer.....	9
Figure 2.4 Molecular mechanism of the thermally induced shape-memory effect	10
Figure 2.5 Various molecular structures of SMPs. A stable network and a reversible switching transition.....	11
Figure 2.6 Shaped morphing wings produced by Lockheed Martin.....	17
Figure 2.7 Snapshots of crack closure and crack rebonding when the sample (l-PCL50:n-PCL50) was unclamped from the Linkam tensile stage and heated to the temperatures shown above (stereo micrographs scale bar: 500 μ m).....	18
Figure 2.8 Depiction of removal of a clot in a blood vessel using the laser-activated SMP microactuator coupled to an optical fiber.(a) The temporary straight rod form. (b) The permanent corkscrew form by laser heating. (c) The deployed microactuator is retracted to capture the thrombus	18
Figure 2.9 A reversible attachment based on SMPs: (a) an alternative SMP based smart hook and loop attachment embodiment; (b) schematics of working process of the active hook-and-loop fastener.....	20
Figure 2.10 The epoxy or oxirane ring structure.	20
Figure 2.11 Chemical structure of DGEBA.....	21
Figure 2.12 Chemical structure of CAE.....	22
Figure 2.13 Chemical structure of novolac epoxy resins	22

Figure 2. 14 General synthesis of benzoxazine monomer and its thermal polymerization	24
Figure 2. 15 Schematic representation of a) monofunctional benzoxazine monomers and b) bifunctional benzoxazine monomers and c) multifunctional benzoxazine monomers.....	25
Figure 2.16 Schematic of synthesis of V-fa.....	26
Figure 2.17 Schematic of synthesis of F-Bz.....	27
Figure 2.18 Schematic of synthesis of S-Bz.....	27
Figure 3.1 Infra-red spectrum over the region from 1000-800 cm^{-1} of the 40% epoxy copolymer after the (a) 25°C, (b) 100°C, (c) 140°C, (d) 160°C, and (e) 205°C stage of cure	28
Figure 3.2 the glass transition temperature of copolymer.	29
Figure 3.3 the flexural strength of copolymer.....	30
Figure 3.4 loss tangent versus temperature of NGDE/PBA-a SMPs at various mole percents of BA-a: (●)30mol%, (■) 35mol%, (◆) 40mol%,(▲) 45mol%, (▼) 50mol%[14].....	31
Figure 3.5 storage modulus versus temperature of NGDE/PBA-a SMPs at various mole percents of BA-a: (●) 30mol%, (■) 35mol%, (◆) 40mol%, (▲) 45mol%, (▼) 50mol% [14].....	32
Figure 3.6 Flexural strength (a) and flexural modulus (b) of the benzoxazine-modified epoxy SMP samples at various compositions at room temperature.....	34
Figure 3.7 Recovery time as a function of BA-a content of the benzoxazine-modified epoxy SMP samples at various composition: (●) T_g , (■) $T_g+20^\circ\text{C}$	35
Figure 3 8 Recovery stress as a function of BA-a content of the benzoxazine-modified epoxy SMP samples at various compositions	36
Figure 3.9 DSC trace of V-fa.....	37

Figure 3.10 TG-MS trace of V-fa.....	37
Figure 3.11 FT-IR spectra of (a) F-Bz and (b) S-Bz benzoxazine monomers.....	39
Figure 3.12 TGA curves of PF-Bz/PS-Bz mixtures with various F-Bz contents in molar ratios (a) 0%, (b) 25%, (c) 50%, (d) 75%, and (e) 100%	40
Figure 3.13 Relationships between ESO or ECO conversion and temperature in the polymerization with 1 wt.-% BPH for 2 h.	41
Figure 4.1 Schematic illustration of the setup for the shape recovery performance test.....	46
Figure 5.1 FTIR spectra : (a) BA-a monomer. (b) E-fa monomer. (c) V-fa monomer	47
Figure 5.2 TGA thermograms of V-fa/ECO copolymers at various weight percentages of ECO: (■) neat poly(V-fa), (▲) 10wt%, (▼) 20wt%, (▲) 30wt%, (◆) 40wt%, (●) 50wt%, (▲) neat ECO.....	49
Figure 5.3 TGA thermograms of E-fa/ECO copolymers at various weight percentages of ECO: (■) neat poly(E-fa), (▲) 10wt% (▼) 20wt%, (▲) 30wt%, (◆) 40wt%, (●) 50wt%, (▲) neat ECO.....	50
Figure 5.4 Storage modulus of V-fa/ECO copolymer at various weight percentages of ECO: (▼) 20wt%, (▲) 30wt%, (◆) 40wt%, (●) 50wt%	52
Figure 5.5 Storage modulus of E-fa/ECO copolymer at various weight percentages of ECO: (▼) 20wt%, (▲) 30wt%, (◆) 40wt%, (●) 50wt%	53
Figure 5.6 Loss modulus of V-fa/ECO copolymer at various weight percentages of ECO: (▼) 20wt%, (▲) 30wt%, (◆) 40wt%, (●) 50wt%	53
Figure 5.7 Loss modulus of E-fa/ECO copolymer at various weight percentages of ECO: (▼) 20wt%, (▲) 30wt%, (◆) 40wt%, (●) 50wt%	54
Figure 5.8 Shape memory behavior of V-fa/ECO SMPs at 40wt% castor oil based epoxy: (a) original shape, (b) temporary shape, and (c) recovered shapes	55

Figure 5.9 Photographs showing various states of bending in shape fixity process for SMP samples: (a) first stage of samples, (b) deformed state of temporary shape at $T_g + 20^\circ\text{C}$ by bending for 10%, and (c) fixed state of temporary shape at room temperature.....	56
Figure 5.10 Photographs showing first stage of E-fa/ECO shape memory polymer system at room temperature.....	57
Figure 5.11 Shape fixity of V-fa/ECO at room temperature as a function of ECO contents at 20wt%, 30wt%, 40wt%, and 50wt%.....	57
Figure 5.12 Series of images showed the shape recovery of the V-fa/ECO SMPs with 50wt% ECO content at $T_g + 20^\circ\text{C}$	59
Figure 5.13 Shape recovery of V-fa/ECO at $T_g + 20^\circ\text{C}$ as a function of ECO contents at 20wt%, 30wt%, 40wt%, and 50wt%.	60
Figure 5.14 Recovery angle as a function of recovery time during the shape recovery process at $T_g + 20^\circ\text{C}$ of the V-fa/ECO SMPs samples at various ECO contents : (▼) 20wt%, (▲) 30wt%, (◆) 40wt%, (●) 50wt%.....	61
Figure 5.15 Shape fixity of V-fa/ECO at ECO content of 40wt% versus deformation cycle	62
Figure 5.16 Shape recovery of V-fa/ECO at ECO content of 40wt% versus deformation cycle	63

LISTS OF TABLE

Table 3.1 Properties of NGDE/PBA-a SMP at various BA-a contents.....	32
Table 3.2 Properties of benzoxazine-modified epoxy SMP samples from DMA.....	33
Table 3.3 Properties of PF-Bz, PS-Bz and their copolymer from DMA.....	40
Table 3.4 Thermal mechanical analysis of the cured ESO/BPH and ECO/BPH systems.	42



CHAPTER I

INTRODUCTION

1.1 Overview

Shape Memory Polymers (SMPs) are known as smart polymer materials which can be deformed and fixed in a temporary shape, from which they recover their original shape only when exposed to an appropriate stimulus [1]. such as, temperature, moisture, pH, electric or magnetic fields [2]. SMPs can be used widely in many areas such as biomedical, self-healing materials and aerospace applications [3]. In some applications, SMPs have been used to substitute shape memory metallic alloys (SMAs) because they possess more advantage including excellent processing, light weight, low cost, easy control of activation temperature and great flexibility [4].

Generally, thermosets are widely used as SMP materials such as epoxy resin is one of the most popular thermoset that have been widely used for coatings, electronic materials, adhesives, and matrices for fiber-reinforced composites because of their outstanding mechanical properties, high adhesion strength, good heat resistance, and high electrical resistance [5]. Shape memory epoxies are the most attractive systems because of the ease of process ability, composite forming properties and dimensional stability. Shape memory epoxy polymers that can be processed into elastic memory composites are candidate materials in the processing of many smart engineering systems [6].

In addition, Rimdusit et al. [7] developed shape memory polymer based on benzoxazine resin (BA-a) alloyed with aliphatic, aromatic epoxy and used Jeffamine D230 as the epoxy curing agent. Enhanced thermo-mechanical performance of the epoxy SMPs was achieved by an addition of the BA-a resin. The incorporation of the BA-a contributed to higher storage modulus in the glassy state, higher crosslink density,

enhanced flexural strength and greater flexural modulus at room temperature than epoxy-based SMPs cured solely by Jeffamine D230. The obtained SMPs also showed excellent shape fixity values of about 98–99% and the recovery stress of the benzoxazine-modified epoxy SMPs was also observed to be larger than that of epoxy-based SMPs.

In recent years, the choice of raw materials are always a key subject of interest to researchers due to concern about the environment, and the alarming rate of consumption of petroleum-based product. Therefore the polymer researchers have shifted toward incorporating natural renewable resources into the production of the majority of synthetic polymer. Apart from traditional Bio-based epoxy resins derived from renewable natural resources have attracted increasingly interest because of their low cost and biodegradability [5]. Vegetable oils are complex multi-component mixtures of different triacylglycerols, i.e., esters of glycerol and fatty acids. Triglycerides containing a large variety of unsaturation sites can be easily epoxidized with organic per acids or H_2O_2 , and epoxidized vegetable oils show excellent potential as inexpensive, renewable materials for industrial applications [8, 9]. Park et al [10] synthesized epoxidized soybean oil (ESO) and epoxidized castor oil (ECO) by reacting soybean or castor oil with glacial acetic acid/ H_2O_2 . The authors also found that, the cured ECO samples showed a higher glass transition temperature (T_g) than those ESO.

Benzoxazine resins are a novel kind of thermosetting phenolic resin that can be synthesized from phenol, formaldehyde and amine group. The curing of the resins involves ring-opening polymerization without a catalyst or a curing agent and does not produce by-products upon curing which results in void-free products. Polybenzoxazines have some reported outstanding properties such as high glass-transition temperature, high thermal stability, near-zero volumetric shrinkage or expansion upon polymerization, low melt viscosity before cure resulting in its high process ability, low water absorption. Furthermore, polybenzoxazines possess high

electrical properties, excellent mechanical performance and wide molecular design flexibility [11-13].

In addition, Tanpitaksit et al [14] investigated effects of benzoxazine resin as a curing agent and a stable network segment on property enhancement of shape memory epoxy. An incorporation of the benzoxazine resin in the aliphatic epoxy based SMP resulted in an increase of glass transition temperature, storage modulus, crosslink density and recovery stress of the SMPs. The obtained SMPs provided an outstanding shape fixity value up to 99% at room temperature and at different active temperatures, i.e. T_g and $T_g + 20^\circ\text{C}$, all SMPs needed only 1–3 minutes to fully recover to their permanent. Therefore, the obtained aliphatic epoxy/ polybenzoxazine SMPs are attractive as shape memory materials to be used in a broad range of applications such as hinge or deployable structure.

Recently, the polymer researchers have shifted toward synthesizing bio-based polybenzoxazine by using natural compounds e.g. cardanol [15, 16], vanillin [17, 18], eugenol [19], furfurylamine [15, 19] and Stearylamine [19], which cardanol is obtained by vacuum distillation of cashew nut shell liquid, vanillin is extracted from the seed pods of *Vanilla planifolia*, eugenol is extracted from cloves, furfurylamine is a green platform product derived from a variety of agricultural by-products such as corncobs and wheat bran and stearylamine can be obtained from vegetable oil.

In addition, N.K. Sini et al. [14] reported a completely renewable monofunctional benzoxazine based on vanillin and furfurylamine. The role of formyl group on the curing behaviour of monomer and the thermal stability of the cross-linked polymer were investigated. A mechanism of polymerization was proposed to account for the highly cross-linked structure of the cured polymer. The renewable benzoxazine showed a low curing temperature, very high T_g and high char yield compared to petroleum based benzoxazines. Thirukumaran et al. [16] synthesized bio-based benzoxazine monomer based on eugenol, furfurylamine and stearylamine (F-Bz and

S- Bz) and investigated characterization, thermal polymerization, and thermo-mechanical properties of these new benzoxazines. The authors also found that, bio-based benzoxazine monomers (F-Bz and S-Bz) have been successfully synthesized by a solventless method from well-known renewable organic resources (eugenol, stearylamine, and furfurylamine). The polymer (PF-Bz) shows the maximum thermal stability when compared with the polymer (PS-Bz) and all the polymers also exhibit good flame retardant properties.

Accordingly, the purpose of this research is to study potential use of bio-based benzoxazine- epoxy (bio-based) copolymers as shape memory polymer and characteristics of bio-based shape memory polymer such as shape fixity, shape recovery, thermal and mechanical

1.2 Objectives

1. To investigate feasibility of bio-based benzoxazine/epoxy based shape memory polymer.
2. To examine characteristics of shape memory polymers from bio-based benzoxazine/epoxy such as shape fixity, shape recovery, thermal and mechanical properties.

1.3 Scope of the study

1. Synthesis of vanillin- furfurylamine- based benzoxazine (V-fa) and eugenol- furfurylamine-based benzoxazine (E-fa) resins by solventless synthesis technology.
2. Preparation of shape memory polymers from bio based V-fa/ECO and E-fa/ECO having 10-50wt% of ECO.
3. Property evaluation of two bio-based benzoxazine/ECO SMPs as follows.
 - 3.1 Chemical structure
 - (Fourier transforms infrared spectrometer)
 - 3.2 Thermal properties

- The degradation temperatures at 5% weight loss (Td5) and char yields at 800°C (Thermogravimetric analyzer)

3.3 Mechanical properties

- Dynamic mechanical properties (Dynamic mechanical analyzer)

3.4 Shape memory properties

- Shape fixity ratio
- Shape recovery ratio
- Recovery time

1.4 Procedure of the study

1. Reviewing related literature.
2. Preparation of chemicals and equipment for using in this research.
3. Synthesis of benzoxazine resin based on vanillin-furfurylamine and eugenol-furfurylamine by a solventless method.
4. Preparation of vanillin-furfurylamine benzoxazine-epoxy based on epoxidized castor oil and eugenol-furfurylamine benzoxazine – epoxy based on epoxidized castor oil shape memory polymers.
5. Determination of thermal, mechanical and shape memory properties of two bio-based poly(benzoxazine-epoxy) as follows:
 - Transition temperature
 - Flexural strength and flexural modulus
 - Shape fixity
 - Shape recovery
 - Recovery time
6. Analysis of the experimental results
7. Preparation of the final report

CHAPTER II

THEORY

2.1 Shape Memory Polymers (SMPs)

The polymer materials have various elasticity from hard one like a glass to soft one like a rubber. The shape memory polymers, however, have the characteristics of both of them, and its elasticity modulus shows reversible change with the glass transition temperature (hereafter called T_g) as the border [1]. The dependence of the elasticity modulus to the temperature is shown in Figure. 2.1. The shape memory polymers, when heated above T_g , get as soft as rubber and is easy to change the shape, and when cooled below T_g , it retains the shape intact (shape fixing characteristic). When heated up again above T_g , the material autonomously returns to the original shape (shape recovery characteristic). The material property which is repeatedly returning back to the original shape is called "shape memory" [20].

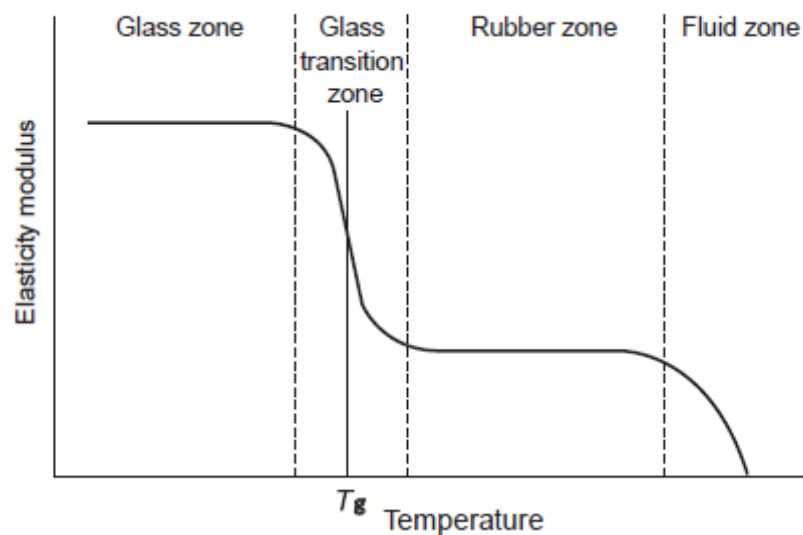


Figure 2.1 Temperature dependency of elasticity modulus of SMP [20]

Shape memory polymers (SMPs) represent responsive polymers which can fix deformed temporary shape and recover their original shape depend on external stimulus. They can be stimulated by temperature, pH, chemicals, and light upon application of an external stimulus, they also have the ability to change their shape. The shape of thermally responsive shape memory polymers can be readily changed above the shape memory transition temperature (T_{trans}) and the deformation can be fixed below this temperature. As a result, when they are heated above T_{trans} their original shape can be recovered automatically.

A typical SMP can be programmed to fix one temporary shape and subsequently recover to its permanent shape upon stimulation (typically heating), as illustrated in Figure. 2.2a. the temporary shape is usually defined by the applied force during the shape fixing step. Accordingly, this step is also called a programming step which programming refers to the external and physical manipulation process that defines the shape shifting pathway. Since the shape memory cycle in Figure.2.2a involved a total of two shapes (one temporary and one permanent), the associated behavior is called a dual-shape memory effect (dual-SME), representing the simplest and most well-known behavior for SMPs.

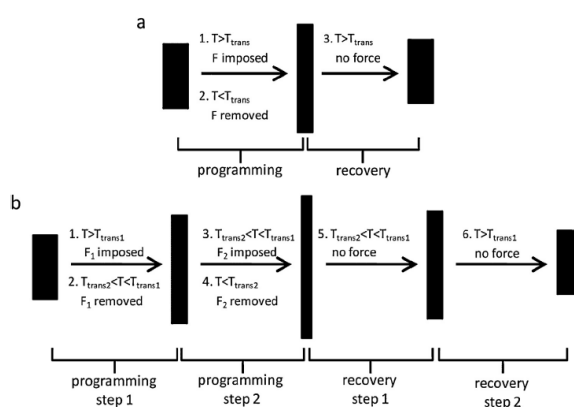


Figure 2.2 Schematic illustrations of (a) Dual-shape memory effect and (b) Triple-shape memory effect [21].

A multi-SMP refers to a polymer that is capable of “memorizing” more than one temporary shape and subsequently recovering in a highly controllable manner. Notably, this definition of multi-SMPs makes no distinction between the so-called triple-SMP (Figure. 2.2b) and an SMP with more than two temporary shapes. It is critical to point out that, in both Figure. 2.2a and b, the shape changing occurs only in one direction, as the arrows indicated. That is, temperature change alone would not drive the recovered shape(s) back to the temporary shape(s). Importantly, this “irreversibility” should be distinguished from reprogramming in that change in both temperature and external stress condition would enable the switch from the recovered shape to the temporary shape. Thus, both the dual- and multi-SMEs discussed in the preceding belong to the so-called one-way (or irreversible) shape memory effect (1W-SME). In contrast, a 2W-SMP can exhibit programmable and reversible shape switching between two (or more) distinct shapes. Here again, “programmable” is the key that distinguishes a 2W-SMP from many common [21]

The shape memory mechanism of SMP is schematically shown in Figure 2.3 and the memory process is illustrated in five steps [22]

- In step 1. A SMP specimen is deformed to its prospective shape when it is heated above transition temperature (T_t) and subject to applied force
- In step 2. The prospective shape of the SMP specimen is kept under the applied force when the specimen is cooled below T_t .
- In step 3. The applied force is removed and the prospective shape is fixed, this process is called shape fixity in shape memory behavior.
- In step 4. Shape memory polymer create a recovery force and the memorized shape is recovered free of mechanical loading when the specimen is heated above T_t .

- In step 5. The SMP specimen is cooled below T_t with its original shape kept.

The same SMP specimen can repetitively undergo the above shape memory process.

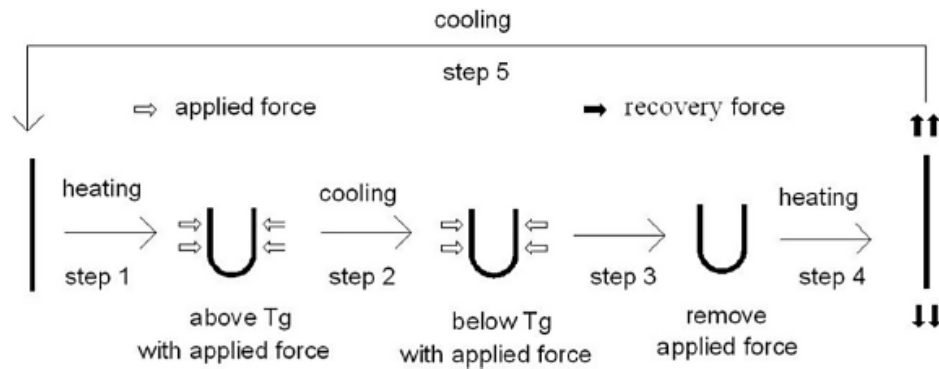


Figure 2.3 Schematic of thermo-mechanical cycle leading to strain recovery for a shape memory polymer [22].

2.1.1 Shape memory effects (SME)

For a polymer to possess shape memory properties, it has to have a permanent network and a reversible phase. Permanent shape can be achieved via chemical crosslinking or physical crosslinking (e.g. chain entanglement and crystallization). The fixing of temporary shapes is due to the reversible phase, which corresponds to either a glass transition or a melting transition. When a reversible thermal phase transition is utilized to fix temporary shapes, the corresponding temperature is typically called the shape memory transition temperature (T_{trans}). Since most polymers possess at least one reversible thermal transition, they can be converted into SMP by introducing a permanent network (e.g. chemical crosslinking).

Shape memory behavior can be observed in various polymer systems which are significantly different in molecular structure, morphology and processing method. In its molecular mechanism, the polymer network consists of molecular switches and net-points (Figure. 2.4). The net-points determine the permanent shape of the polymer network and can be of a chemical (covalent bonds) or physical (intermolecular

interactions) nature. Physical cross-linking is obtained in a polymer whose morphology consists of at least two segregated domains, as found for example in block copolymers. Here, domains related to the highest thermal transition temperature (T_{perm}) act as net-points (a hard segment), while chain segments in domains with the second highest thermal transition T_{trans} act as molecular switches (a switching segment). If the working temperature is higher than T_{trans} , then the switching domains are flexible, resulting in an entropic elastic behavior of the polymer network above T_{trans} . If the sample has been previously deformed by application of an external stress, it snaps back into its initial shape once the external stress is released. The molecular mechanism of the shape-memory effect is illustrated for the thermally induced shape-memory effect in Figure. 2.4. The shape-memory polymer network consists of covalent net-points and switching segments based on a physical interaction [23]

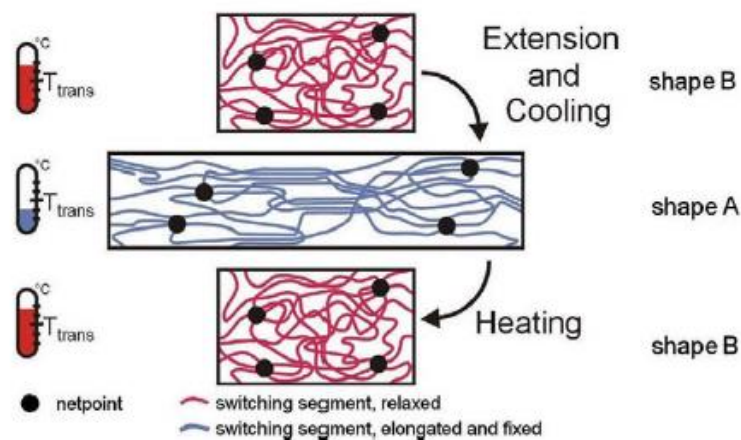


Figure 2.4 Molecular mechanism of the thermally induced shape-memory effect
 T_{trans} = thermal transition temperature related to the switching phase [23].

A stable polymer network and a reversible switching transition of the polymer are the two pre-requisites for the shape memory effect (SME) (Figure. 2.5). The stable network of SMPs determines the original shape, which can be formed by molecule

entanglement, crystalline phase, chemical cross-linking, or interpenetrated network. The lock in the network represents the reversible switching transition responsible for fixing the temporary shape, which can be crystallization/melting transition, reversible molecule cross-linking, and supramolecular association/disassociation [24]

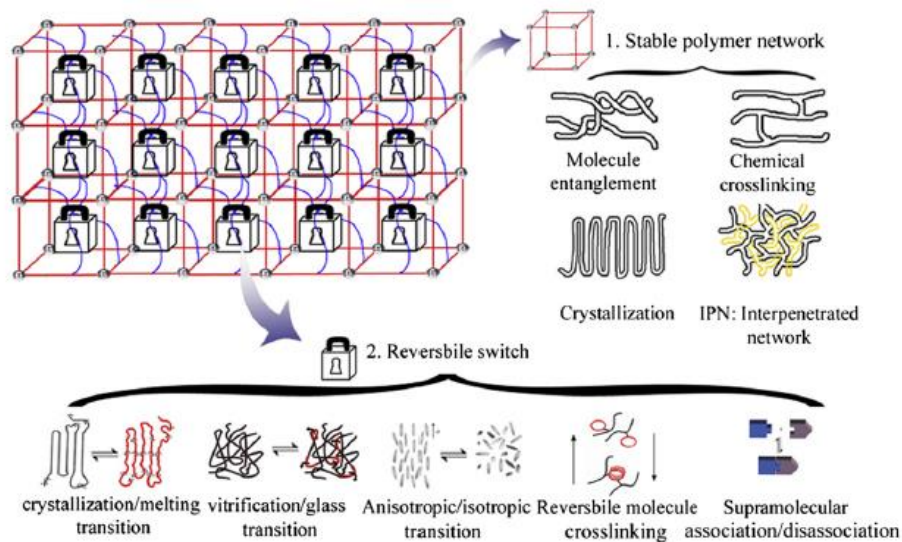


Figure 2.5 Various molecular structures of SMPs. A stable network and a reversible switching transition [24].

2.1.2 Class of shape memory polymers

The following sections will provide a detailed overview on the engineering properties of different classes of SMPs namely the two thermal transitions of a distinct block/component of the SMPs and the melting temperature as well as the glass transition temperature. The melting transition can be applied in chemical-crosslinked rubbers, in semicrystalline polymer networks as well as in physical-crosslinked polymers. Similarly, the glass transition temperature can be applied in chemical-crosslinked thermosets and physical-crosslinked thermoplastics [3]

2.1.2.1 Shape memory polymers based on a melting transition

One possibility for the fixation of the second phase is its

crystallization. The melting of this phase will lead to the shape recovery of the SMP. Often based on chemically cross-linked semi-crystalline networks or (multi)block copolymer systems these materials feature a higher stiffness than other SMP materials as well as a fast shape recovery [3]. However, generally $T_{m\text{-based}}$ possess low thermal and mechanical properties.

2.1.2.2 Shape memory polymers based on a glass transition

Polymeric materials with a glass transition temperature (T_g) above room temperature can be utilized for $T_{g\text{-based}}$ SMPs. These include chemically cross-linked glassy thermosets and physically cross-linked thermoplastics. Within this context a large variety of different materials have been investigated. In comparison to the T_m -based SMPs, the $T_{g\text{-based}}$ SMPs reveal a slower shape recovery due to the broad glass transition (representing a second order phase transition). Therefore, these SMPs are not best choice for applications where a sudden shape recovery is required. But on the other hand, the slow recovery makes them interesting candidates certain for biomedical applications [3]

2.1.3 Parameters for Characterization of SMPs [25]

To characterize the shape memory properties of polymers, a set of parameters is needed. First, the parameters should be able to reflect the nature of polymers. Second, to distinguish them from other properties of materials, shape memory properties are shown through a series of thermo-mechanical cyclic processes. Therefore the parameters should be able to define the whole shape memory processes as well. At last, the design of the parameters should consider the potential applications. The parameters are introduced in the following.

2.1.3.1 Shape fixity

Shape fixity is parameter that described how well to fixed in temporary shape. The sample is first heated to a deformation temperature, normally

(but not always) above T_{trans} , a force is then applied. When a shape memory polymer is activated to a temperature above the transition temperature for triggering typical shape memory behaviors such as T_g , it can develop large deformations which can be fixed by cooling to a low temperature. The shape fixity is the amplitude ratio of the fixed deformation to the total deformation, which is given by shape fixity related to both structures of polymers and the thermo-mechanical conditions of shape memorization. Compared to the macro structures of SMPs, the thermo-mechanical conditions play important roles in determining the shape fixity and other shape memory properties in polymer.

$$\text{Shape fixity} = \frac{\text{Fixed deformation}}{\text{Total deformation}} \times 100$$

2.1.3.2 Shape recovery

A given SMP holding a deformation by low temperature can restore its original shape by being heated up above T_g . Shape recovery is used to reflect how well an original shape has been memorized. Compared with the case of shape fixity, the diverse and confused usages take place not only to notation but also to mathematical expressions for this parameter.

Like shape fixity, shape recovery depends on both the structures of polymers and the thermo-mechanical conditions of shape memorization.

2.1.3.3 Recovery stress

Recovery stress stems from the elastic recovery stress generated in the deformation process. When SMPs are heated and deformed, the elastic stress is generated and the elastic stress is stored when SMPs are cooled below T_g . If the deformed and fixed SMPs are reheated above T_g , the stress stored in SMPs is released as shape recovery stress. In this sense, one cycle of shape memorization can be looked

on as a thermo-mechanical cycle consisting of stress generation, stress storage, and stress release. SMPs are considered promising in development of smart actuators. The characterization of shape recovery stress is therefore essential. The dilemma for the characterization of recovery stress of SMPs is chiefly caused by viscoelasticity of polymers, especially for the thermoplastic SMPs. Owing to the limitations of equipment and efficiency of heat transfer, it is practically impossible to heat or cool an SMP to a certain temperature in a sufficiently short time in experiments. Therefore the stress relaxation is inevitable by all means if only the SMP is in a constrained state. As a consequent, the stress generated in deformation must be lost more or less in the shape fixing and shape recovery processes. Additionally, the rate of stress relaxation alters with the temperature change in the whole shape memory process, which means that its influence on the recovery stress is unknown. In the other words, the recovery stress may change all the time with the stress relaxation, but the exact nature of the change is uncertain. Therefore it is difficult to calculate the recovery stress in quantitative terms.

2.1.3.4 Recovery rate

This parameter is a dimension for describing the speed when a given SMP recovered from a temporary shape to its original shape by being heated. The parameter has no uniform name, which called were as speed of recovery process, deformation recovery speed or shape recovery speed. The parameter can be measured qualitatively and quantitatively.

$$\text{Recovery rate} = \frac{\text{Deformation recovered by sample in reheating process}}{\text{Fixed deformation}} \times 100$$

2.1.4 Applications of Shape Memory Polymer

The potential applications for SMPs that include smart clothing, space

and medical applications, smart structural repair, reconfigurable tooling, micro-electromechanical systems, actuators, self-healing, health monitoring, biomedical devices, self-repairing auto bodies, kitchen utensils, switches, sensors, intelligent packing, heat-shrinkable tubes, and biosensors. Specific examples from recent works are detailed from now on.

2.1.4.1 Deployable structures

For the traditional aerospace deployable devices, the change of structural configuration in-orbit is accomplished through the use of a mechanical hinge, stored energy devices or motor driven tools. There are some intrinsic drawbacks for the traditional deployment devices, such as complex assembling process, massive mechanisms, large volumes and undesired effects during deployment. In contrast, the deployment devices fabricated using SMPs and their composites may overcome certain inherent disadvantages.

2.1.4.2 Morphing structures

In morphing structures application can apply in some flight. The flight vehicles are envisioned to be multi-functional so that they can perform more missions during a single flight, such as an efficient cruising and a high maneuverability mode. When the airplane moves towards other portions of the flight envelope, its performance and efficiency may deteriorate rapidly. To solve this problem, many researchers have proposed to radically change the shape of the aircraft during flight. By applying this kind of technology, both the efficiency and flight envelope can be improved. This is because different shapes correspond to different trade-offs between beneficial characteristics, such as low energy consumption, speed and dexterity [23]. For instance, the morphing structure technology to demonstrate radical shape changes was developed by Defense Advanced Research Projects Agency (DARPA). As illustrated in Figure 2.6, Lockheed Martin also achieves a z-shaped morphing change in flight model [26]

Typically, a wing skin is great necessary for a morphing aircraft. Researchers always focus their works on investigating suitable types of materials that are currently available to be used as a skin material for a morphing wing. In this case, the SMPs show more advantages for morphing application. It becomes flexible when heated to a certain degree. Then it returns to a solid state when the external stimulus is terminated. Since SMPs holds the ability to change its elastic modulus, they could potentially be used in the mentioned concept morphing aircraft designs [26].

Although shape memory alloys are commercially available and found a wide range of different applications. However, SMPs have one decisive advantage, particularly considering applications in aerospace: Their weight. The weight of the applied materials is one of the most crucial issues in the design of new systems in aerospace (e.g., the newest Boeing 787 Dreamliner utilizes >50% polymer composites in the primary structure). Consequently, enormous efforts have been undertaken in the development of new SMPs for aerospace applications. The field for potential applications in this sector is huge [26].

Although shape memory alloys are commercially available and found a wide range of different applications. However, SMPs have one decisive advantage, particularly considering applications in aerospace: Their weight. The weight of the applied materials is one of the most crucial issues in the design of new systems in aerospace (e.g., the newest Boeing 787 Dreamliner utilizes >50% polymer composites in the primary structure). Consequently, enormous efforts have been undertaken in the development of new SMPs for aerospace applications. The field for potential applications in this sector is huge [3].



Figure 2.6 Shaped morphing wings produced by Lockheed Martin [3, 26]

2.1.4.3 Self-healing materials

The ability to repair a mechanical damage is a fascinating property of self-healing materials. The SME can enhance the self-healing ability of polymeric materials, which is referred to as shape-memory assisted self-healing (SMASH). In that case, the SME enhances the self-healing process by bringing the crack surfaces closer together. SMASH system was prepared by Mather et al [27] which they designed an interpenetrating network consisting of high molar mass linear PCL and reversibly crosslinked PCL. The latter was synthesized by a thiolene reaction of PCL-diacrylate with pentaerythritoltetrakis-(3-mercaptopropionate) and provides the shape-memory behavior. On the other hand, the high molar mass linear PCL can re-entangle after diffusion and, thus, is used as the healing agent. The self-healing efficiencies of different mixtures were tested, showing that complete healing is possible if the content of linear PCL is at least 25 wt% (Figure. 2.7).

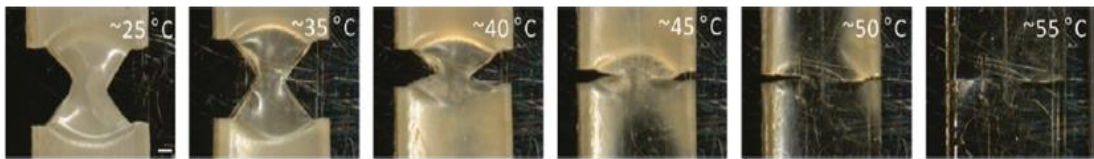


Figure 2.7 Snapshots of crack closure and crack rebonding when the sample (l-PCL50:n-PCL50) was unclamped from the Linkam tensile stage and heated to the temperatures shown above (stereo micrographs scale bar: 500 μm) [27].

2.1.4.4 Biomedicine and bio inspiration

An attractive application area for SMPs is use in medical device. SMPs show extensive interest in used for biomaterials and bio inspiration. For instant, polyurethane SMP performs excellent biocompatibility, and it can be used for the deployment of different clinical devices when contacted or implanted in the human body [26].

The same working principle can also be utilized for the design of vascular stents based on shape memory polymers. The state of the art is the utilization of stents made of stain-less steel or other metal containing materials (e.g., several alloys). Several drawbacks of these stents, such as too high stiffness for navigation.

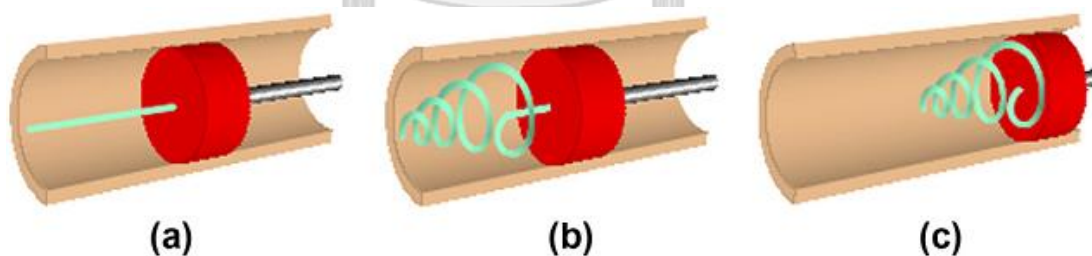


Figure 2.8 Depiction of removal of a clot in a blood vessel using the laser-activated SMP microactuator coupled to an optical fiber. (a) The temporary straight rod form. (b) The permanent corkscrew form by laser heating. (c) The deployed microactuator is retracted to capture the thrombus [23].

2.1.4.5 Automobile [28]

SMPs have been used in automobile engineering, and many interesting products have been developed. Some interesting applications of SMPs include seat assemblies, reconfigurable storage bins, energy-absorbing assemblies, tunable vehicle structures, hood assemblies, releasable fastener systems, airflow control devices, adaptive lens assemblies and automotive body molding. The reasons for using SMPs are due to their excellent advantages such as shape memory behavior, easy manufacturing, high deformed strain and low cost. That is why they have attracted a lot of attention in automobile engineering and have even been used to replace the traditional structural materials, actuators or sensors.

As a typical example, SMPs are proposed to be used for the reversible attachments, as shown in Figure. 2.9. In this embodiment (Figure. 2.9a), one of the two surfaces to be engaged contains smart hooks, at least one portion of which is made from SMPs materials. By actuating the hook and/or the loop, the on-demand remote engagement and disengagement of joints/attachments can be realized (Figure. 2.9b). With a “memorized” hook shape, the release is effective and the pull-off force can be dramatically reduced by heating above the T_g . It can be used for a reversible lockdown system in the lockdown regions between the vehicle body and closure.

SMPs can also be used in an airflow control system to solve a long-time problem for automobiles. As we know, airflow over, under, around, and/or through a vehicle can affect many aspects of vehicle performance, including vehicle drag, vehicle lift and down force, and cooling/heating exchange. Reduction to vehicle drag reduces the consumption of fuel. A vehicle airflow control system, which comprises an activation device made of SMP material, actively responds to the external activation signal and alters the deflection angle accordingly. Thus, the airflow is under control based on the environmental changes.

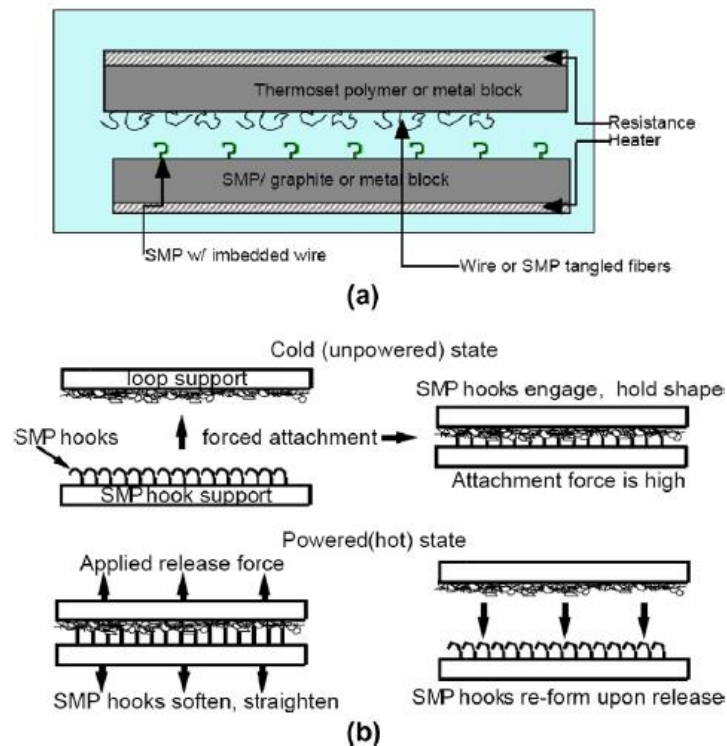


Figure 2. 9 A reversible attachment based on SMPs: (a) an alternative SMP based smart hook and loop attachment embodiment; (b) schematics of working process of the active hook-and-loop fastener [26].

2.2 Epoxy Resin

Epoxy resins are thermosetting resins, which are characterized by the presence of an oxirane or epoxy ring, shown in Figure. 2.10. This is represented by a three-member ring containing an oxygen atom that is bonded with two carbon atoms already united in some other way.

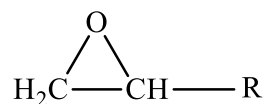


Figure 2.10 The epoxy or oxirane ring structure [5].

The outstanding physical properties exhibited by epoxy resins include [28].

- Low cure shrinkage

- No volatiles given off during cure
- Compatibility with a great number of materials
- Strength and durability
- Adhesion
- Corrosion and chemical resistance
- Electrical insulation.

2.2.1 Synthesis of epoxy resins

2.2.1.1 Bisphenol-A epoxy resins

The most common commercial epoxy resin is formed from the reaction of bisphenol A and epichlorohydrin, in the presence of a basic catalyst. This resin is known as the diglycidyl ether of bisphenol A (DGEBA). Figure 2.11 shows the chemical structure of DGEBA. The properties of the DGEBA resin depend on the number of repeating units. Low-molecular-weight molecules tend to be liquids and higher-molecular-weight molecules tend to be more-viscous liquids or solids [5].

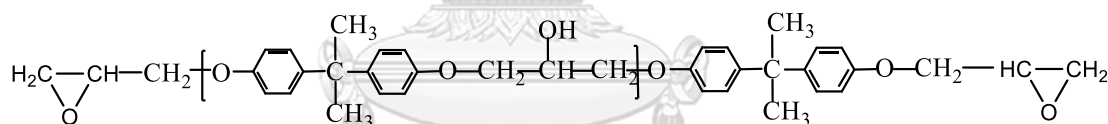


Figure 2.11 Chemical structure of DGEBA [5].

The low-MW, liquid epoxy resins are generally the most desirable to use in adhesive formulations because of easier compounding capability and application via liquid dispensers. They also have relatively high reactivity and crosslink density.

Solid, higher-MW epoxy resins are often used for adhesive formulations that are applied as solids (e.g., film and powder) or a solvent solution. The higher-MW DGEBA resins are also used where improved toughness, flexibility, and adhesion are required. These resins have a greater number of hydroxyl groups along the chain and, thus, can provide better adhesion and additional reaction mechanisms [28].

2.2.1.2 Cycloaliphatic epoxy resins

The cycloaliphatic epoxy resin (CAE), 3',4'-epoxycyclohexyl-methyl 3,4-epoxycyclohexanecarboxylate is synthesized from the epoxidation of olefinic compounds. The epoxidation process involves the use of an olefinic or polyolefinic compound and a peracid (e.g., peracetic acid) or other oxidizing substances such as hydrogen peroxide, molecular oxygen, or even air. Cycloaliphatic epoxy resins are almost water-white, very low-viscosity liquids. They provide excellent electrical properties such as low dissipation factor and good arc-track resistance, good weathering, and high heat distortion temperature [28]. The chemical structure of CAE is shown in Figure 2.12.

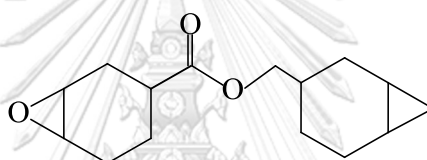


Figure 2.12 Chemical structure of CAE [5].

2.2.1.3 Novolac epoxy resins

Novolac epoxy resins are glycidyl ethers of phenolic novolac resins that have been synthesized by reacting phenolic novolac resin with epichlorohydrin. Figure 2.13 shows the chemical structure of novolac epoxy resins.

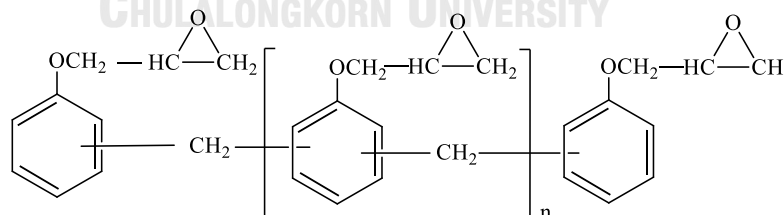


Figure 2.13 Chemical structure of novolac epoxy resins [5].

The novolac epoxies are high-viscosity liquids or semisolids, and they are often mixed with other epoxy resins to improve handling and formulation properties. They have much greater functionality than conventional DGEBA resins, and the increased

crosslink density results in greater temperature and chemical resistance. However, novolac epoxies also form very rigid and brittle polymers when fully cured because of their high crosslink density. For this reason, they are often used as modifiers in epoxy adhesive systems rather than as the base polymer [28].

2.2.1.4 Biobased epoxy resins

Polymers derived from renewable natural resources, such as carbohydrates, starch, proteins, fats, and oils, have attracted increasingly interest because of their low cost and biodegradability. Bio-based epoxy can also be obtained using plant oils and fatty acids. Vegetable oils are complex multi-component mixtures of different triacylglycerols, i.e., esters of glycerol and fatty acids. Triglycerides containing a large variety of unsaturation sites can be converted into epoxidized oils using performic acid and peroxide or through enzymatic processes.

Vegetable oils, such as castor, soybean, linseed, palm, hemp, corn, canola and tung oil are an important raw material for the synthesis of biopolymers. Because epoxidized plant-based monomers possess epoxide functional groups along their backbone chains and exhibit the ability to make a three-dimensional elastomeric network when being cured with respective hardeners. On the other hand, these are known to be nontoxic and rigid. These could easily replace petroleum-based epoxy monomers. Moreover, a number of hydroxyl groups present in plant-based epoxy monomers which offer good adhesion between matrix and reinforcement, resulting towards high toughness, good thermal stability, improves dielectric properties, and less moisture absorption[29].

Castor oil (CO) is obtained from the seeds of the CO plant *Ricinus communis* and is a low-cost vegetable oil. The CO being longer shelf life and reasonably low toxicity, easy availability and its exclusive functionality makes it superior above other vegetable oils.

2.3 Benzoxazine Resin

Benzoxazine resins are basically synthesized from phenoxide group, amine functional group, and formaldehyde, thus rendering them tremendous flexibility in their molecular design. The various molecular structures of benzoxazine resins are obtained by using various phenols and amines with different substitution groups attached which these substituting groups can provide additional polymerizable sites and also affect the curing process. Benzoxazine resin can be polymerized by heating. They do not need catalyst or curing agent for polymer curing process.

Polybenzoxazine is a phenolic polymer in which synthesized by the Mannich-like condensation. It can be prepared by using solvent less synthesis technology [30, 31]

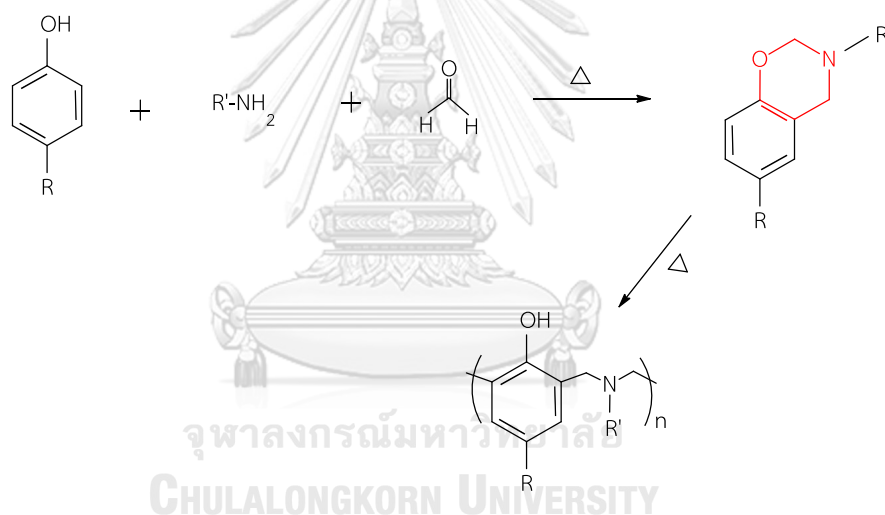


Figure 2.14 General synthesis of benzoxazine monomer and its thermal polymerization [32].

Polybenzoxazines offer many advantages such as low melt viscosity, high glass transition temperature, high thermal stability, good mechanical strength and modulus, low water absorption, low dielectric constant, good adhesive properties, and high resistance to burning and chemical. Polybenzoxazines could be classified by their functionality into monofunctional benzoxazine monomers, bifunctional benzoxazine

monomers, and multifunctional benzoxazine monomers. Several structures of benzoxazine resins have intensively been synthesized by scientists to tailor their properties [11]

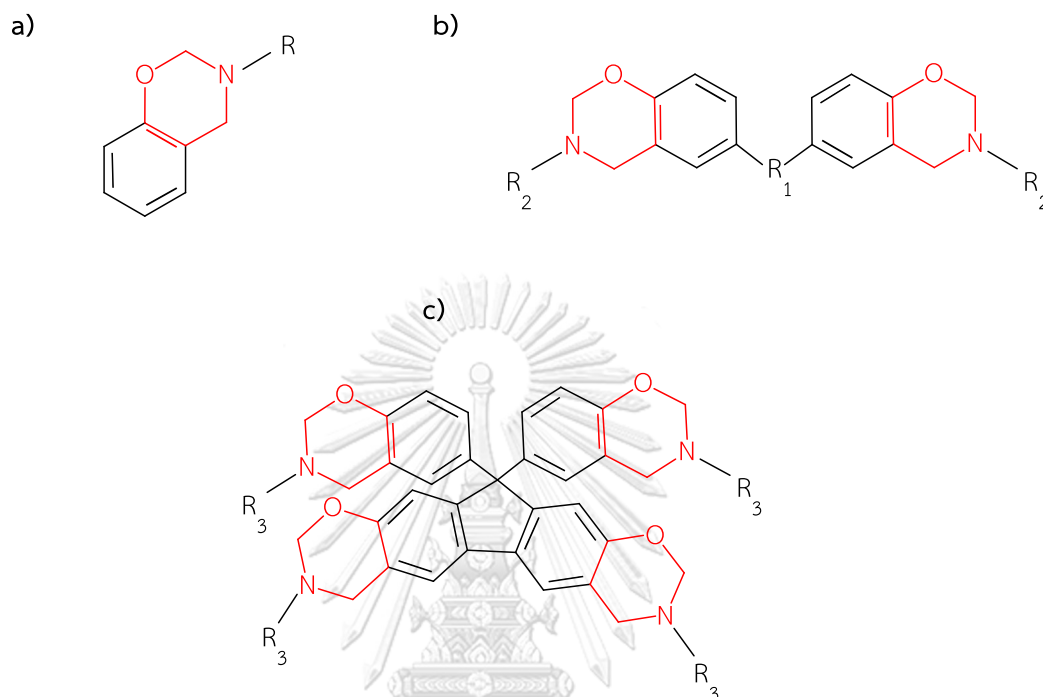


Figure 2.15 Schematic representation of a) monofunctional benzoxazine monomers and b) bifunctional benzoxazine monomers and c) multifunctional benzoxazine monomers [33].

2.3.1 Bio-based benzoxazine

2.3.1.1 Vanillin-based benzoxazine

Vanillin, 4-hydroxy-3-methoxybenzaldehyde, is most prominent as the principal flavor and aroma compound in vanilla which it is extracted from the seed pods of Vanilla. In green seed pods, vanillin is a naturally occurring phenol containing a methoxy group and a formyl group.

Sini et al. [17] investigated the synthesis, polymerization mechanism, and thermal properties of vanillin-furfurylamine-based benzoxazine (V-fa). The schematic of synthesis of V-fa is shown in Figure 2.16

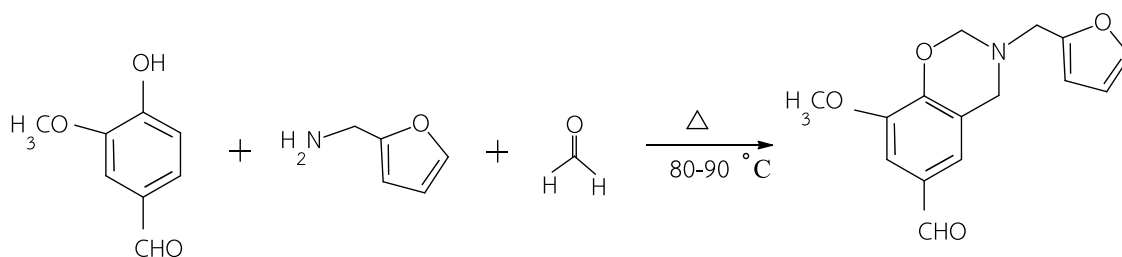


Figure 2.16 Schematic of synthesis of V-fa [17].

V-fa showed the ring-opening polymerization of oxazine ring at low temperature (170-190 °C). The poly (V-fa) showed high glass transition temperature (270 °C), the decomposition temperature at 5% mass loss (T_{d5}) was 351 °C and the char yield at 800°C was 65%, which is attributed to the high cross-linking density.

2.3.1.2 Eugenol-based benzoxazine

Eugenol (4-allyl-2-methoxyphenol) is a phenolic compound containing an allyl group and a methoxy group, which is the main component in the essential oil extracted from clove.

Thirukumaran et al [19] studied synthesis two benzoxazine monomer from naturally occurring sources, i.e., eugenol (an extraction from clove), furfurylamine, stearylamine, and paraformaldehyde which a solvenless method was adopted to synthesize benzoxazine monomer. The schematic of synthesis of eugenol-furfurylamine-based benzoxazine monomer (F-Bz) and eugenol-stearylamine-based benzoxazine monomer (S-Bz) are shown in Figure 2.17 and Figure 2.18

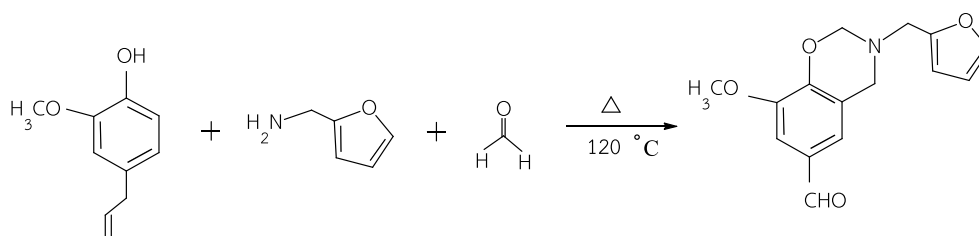


Figure 2.17 Schematic of synthesis of F-Bz [19].

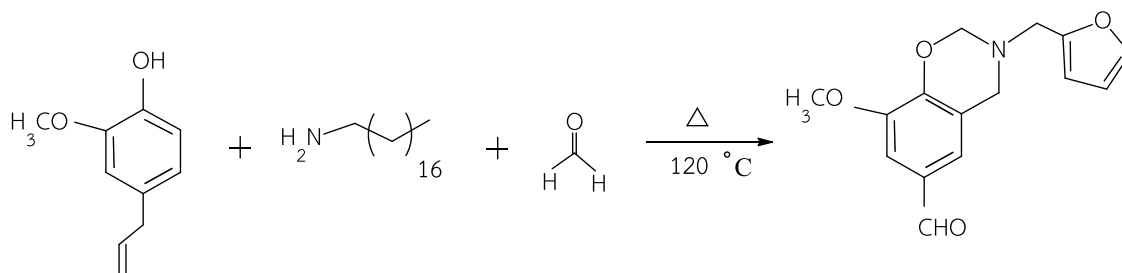


Figure 2.18 Schematic of synthesis of S-Bz [19].

The structures of the monomers were supported by FT-IR, ¹H NMR, ¹³C NMR, and HR-MS spectra, which showed the existence of a reactive benzoxazine ring. The storage modulus, crosslink density and glass transition temperature (T_g) of PF-Bz were 3.33 GPa, 4.4 mol m⁻³ and 148 °C, respectively which were higher than PS-Bz due to the rigid molecular stuture more than PS-Bz and the PF-Bz shown the hight thermal stability when compared with PS-Bz.

CHAPTER III

LITERATURE REVIEW

Ishida, H. , Allen, D. J. , (1996) investigated mechanical characterization of copolymer based on benzoxazine and epoxy (DGEBA). The benzoxazines are copolymerized with an epoxy resin in order to modify their performance. The addition of epoxy to the polybenzoxazine network greatly increases the crosslink density of the thermosetting matrix and strongly influences its mechanical properties. Copolymerization leads to significant increases in the glass transition temperature, and flexural stress. Benzoxazine-epoxy copolymers may be produced without the use of an external curing agent by the coreaction of a polybenzoxazine precursor with the diglycidyl ether of bisphenol-A. It is believed that the copolymerization reaction occurs via the opening of the epoxide ring by the phenolic hydroxyl functionalities present in the polybenzoxazine precursor.

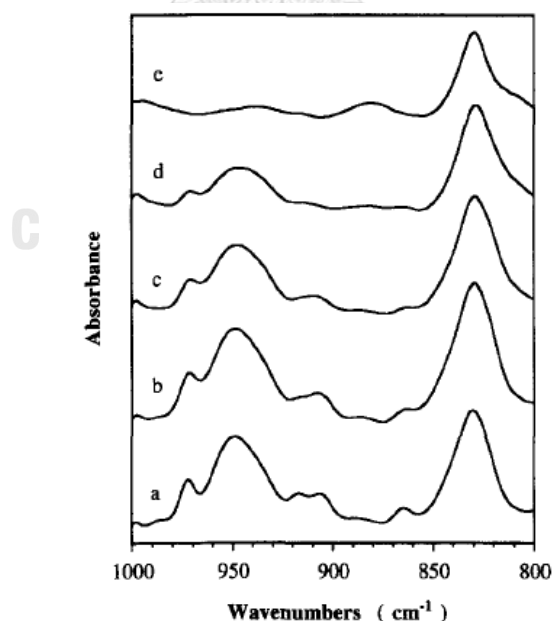


Figure 3.1 Infra-red spectrum over the region from 1000-800 cm⁻¹ of the 40% epoxy copolymer after the (a) 25°C, (b) 100°C, (c) 140°C, (d) 160°C, and (e) 205°C stage of cure [34]

Figure 3.1 show the stage of cure which the consumption of epoxy can be monitored by the 913 cm^{-1} and 864 cm^{-1} epoxide ring modes that disappear as the ring is opened. The epoxide peaks appear to have almost completely disappeared by the end of the $160\text{ }^{\circ}\text{C}$ stage of cure.

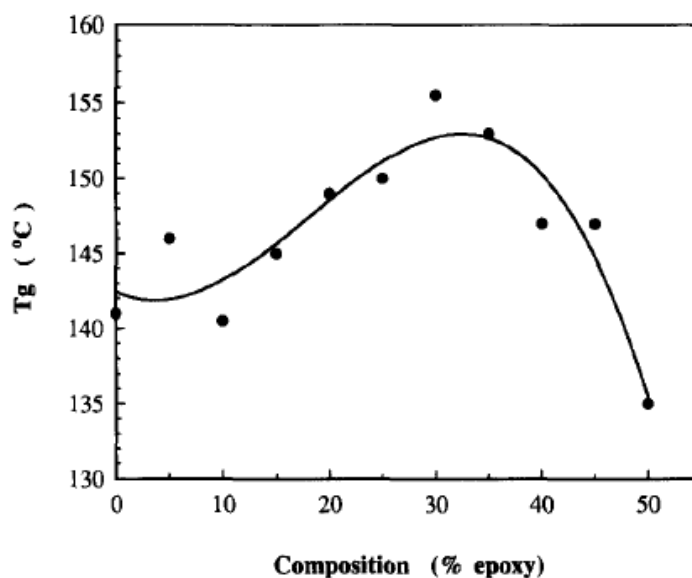


Figure 3.2 the glass transition temperature of copolymer [34].

Figure 3.2 show the glass transition temperature of copolymer. Initially, the incorporation of epoxy in the benzoxazine matrix has the effect of increasing the glass transition temperature of the material over the pure polybenzoxazine. The highest T_g , $156\text{ }^{\circ}\text{C}$, is demonstrated by the material containing 30% epoxy. Beyond 45% epoxy, the copolymers experience a sharp decrease in T_g , with the material containing equal amounts of benzoxazine and epoxy exhibiting a T_g lower than that of the pure polybenzoxazine. The epoxy rich samples, those with greater than about 45% epoxy, show poor mechanical properties due to the fact that the phenolic groups generated by the oxazine ring opening reaction not only serve to catalyse the copolymerization, but also participate as reactants and therefore are consumed by the reaction. Thus, as

the stoichiometric ratio of components is approached, unreacted or small molecular weight epoxy molecules may remain and interfere with network formation or act as a plasticizer.

Figure 3.3 show the flexural strength of copolymer which flexural strength increases linearly as epoxy is incorporated into the benzoxazine network structure.

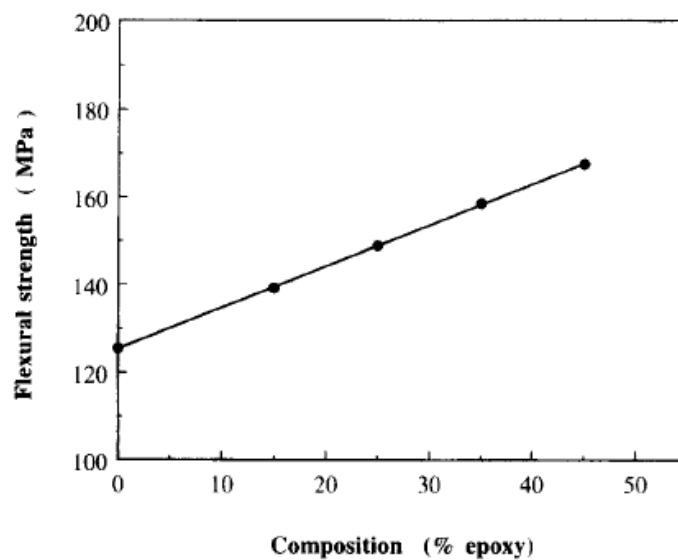


Figure 3.3 the flexural strength of copolymer[34].

Tanpitaksit et al. (2015) investigated effects of bisphenol-*A*/aniline based benzoxazine resin (BA-a) on property enhancement of shape memory epoxy. A suitable content of BA-a in the aliphatic epoxy (NGDE)/polybenzoxazine (PBA-a) samples for good shape memory performance is in a range of 30 to 50 mol%. The storage modulus of the obtained NGDE/PBA-a shape memory polymers (SMPs) was increased from 3.57 GPa for 30 mol% BA-a content to 4.50 GPa for 50 mol% BA-a content. Glass transition temperature of the sample was also substantially increased with increasing BA-a fraction (from 51 °C to 140 °C). Flexural modulus and flexural strength at room temperature of the samples at 50 mol% BA-a were found to be as high as 3.97 GPa

and 132 MPa compared to the maximum values of 2.54 GPa and 100 MPa of SMP based on cyanate ester-epoxy. All samples exhibited a high value of shape fixity close to 100%. A presence of the BA-a in the samples also discovered a greater recovery stress ranging from 0.25 to 1.59 MPa.

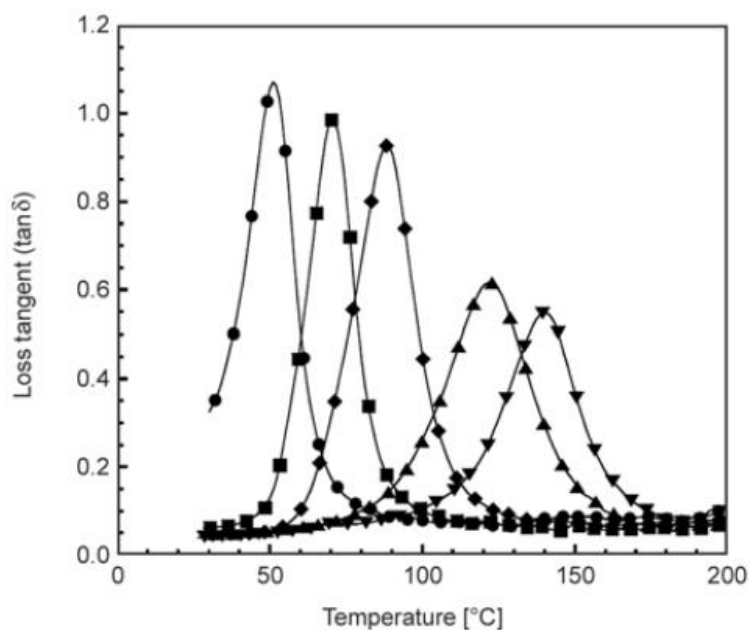


Figure 3.4 loss tangent versus temperature of NGDE/PBA-a SMPs at various mole percents of BA-a: (●)30mol%, (■) 35mol%, (◆) 40mol%,(▲) 45mol%, (▼) 50mol%[14]

Loss tangent ($\tan \delta$) curves from a DMA experiment of the NGDE/PBA-a SMPs at various BA-a contents are depicted in Figure 3.4. The peak positions of the $\tan \delta$ were used to indicate T_g of the samples. We can see that, an increase of the BA-a content in the NGDE/PBA-a SMPs resulted in a systematic increase in the T_g of the samples. This behavior was attributed to the more rigid molecular structure of the polybenzoxazine compared to the epoxy.

The storage modulus at a glassy state (35°C) of the NGDE/PBA-a SMPs are shown in Figure 3.5. From the results, the storage modulus of the samples tended to

increase with increasing BA-a content. The phenomenon is attributed to the addition of the more rigid molecular segments of the PBA-a in the NGDE/PBA-a shape memory samples.

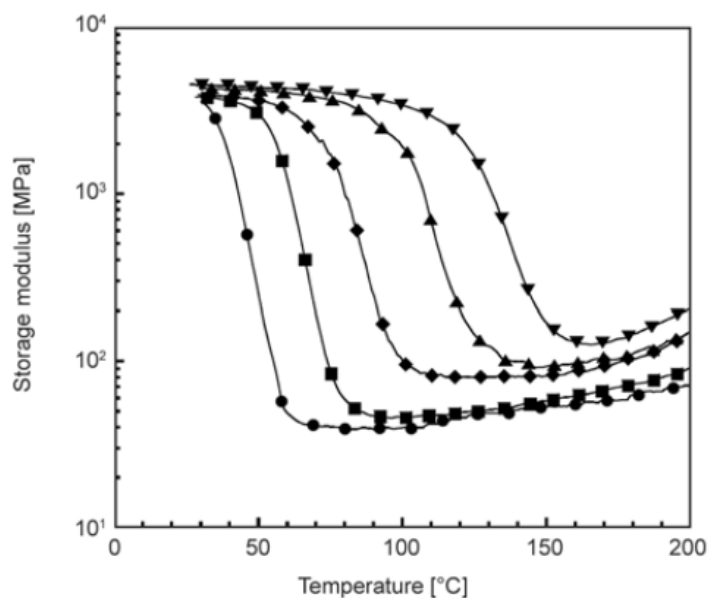


Figure 3.5 storage modulus versus temperature of NGDE/PBA-a SMPs at various mole percents of BA-a: (●) 30mol%, (■) 35mol%, (◆) 40mol%, (▲) 45mol%, (▼) 50mol% [14]

Table 3.1 Properties of NGDE/PBA-a SMP at various BA-a contents

Sample	Flexural strength (MPa)	Flexural modulus (GPa)	Recovery stress (MPa)	Shape fixity at room temp. (%)
BA-a 30 mol%	52	1.6	0.25	99.30
BA-a 35 mol%	78	2.4	0.39	99.10
BA-a 40 mol%	108	3.4	0.62	98.80
BA-a 45 mol%	124	3.8	0.98	98.50
BA-a 50 mol%	132	4.0	1.59	98.10

The properties of this system are presented in Table 3.1. It can be seen that the flexural strength of the samples increased with an increase in amount of the BA-a due to the the addition of high flexural strength PBA-a and chemical linkage formation between PBA-a with the epoxy network. Moreover the flexural modulus of the samples increased with an increase in amount of the BA-a too. Because of the addition of the more rigid PBA-a in to the more flexible aliphatic epoxy as well as an enhanced crosslink density of the obtained polymer network described previously. The recovery stress under flexural mode could be increased with increasing BA-a contents from 0.25 MPa at 30 mole% to 1.59 MPa at 50mol%. In addition, the shape fixity of all ratios is similar values.

Rimduisit et al. (2013) studied effects of benzoxazine resin (BA-a) content on the thermal, mechanical and shape memory properties of epoxy-based shape memory polymers (SMPs). Specimens consisting of aromatic epoxy (EPON 826), aliphatic epoxy (NGDE), Jeffamine D230 and BA-a benzoxazine monomer which they were represented by E, N, D, B, respectively were evaluated. As show in Table 3.2

Table 3.2 Properties of benzoxazine-modified epoxy SMP samples from DMA.

Sample	Storage modulus, E' (GPa) at 35 °C	Crosslink density (mol cm ⁻³)	Glass transition temperature, T _g (°C)
ENDB 1/1/1/0	3.18	2.90 × 10 ⁻³	47
ENDB 1/1/0.8/0.2	3.90	3.25 × 10 ⁻³	72
ENDB 1/1/0.6/0.4	4.34	3.62 × 10 ⁻³	80
ENDB 1/1/0.4/0.6	4.44	3.79 × 10 ⁻³	85
ENDB 1/1/0.2/0.8	4.62	3.81 × 10 ⁻³	92
ENDB 1/1/0/1	4.70	4.29 × 10 ⁻³	120

The digits after the notation give the molar ratio of the monomer in the same order. The increasing of storage modulus and crosslink density were found when increase BA-a content in the alloys as a result of the more rigid characteristics of the BA-a resin. Moreover, the glass transition temperature also increases when increasing of BA-a content due to the more rigid molecular stuture and possibly much higher intramolecular and intermolecular forces in the benzoxazine fraction which can also enhance the T_g of the resulting hybrid polymer network.

The obtained SMPs exhibited a higher flexural strength and flexural modulus than those of the unmodified epoxy-based SMP at room temperature, as seen in Figure 3.6

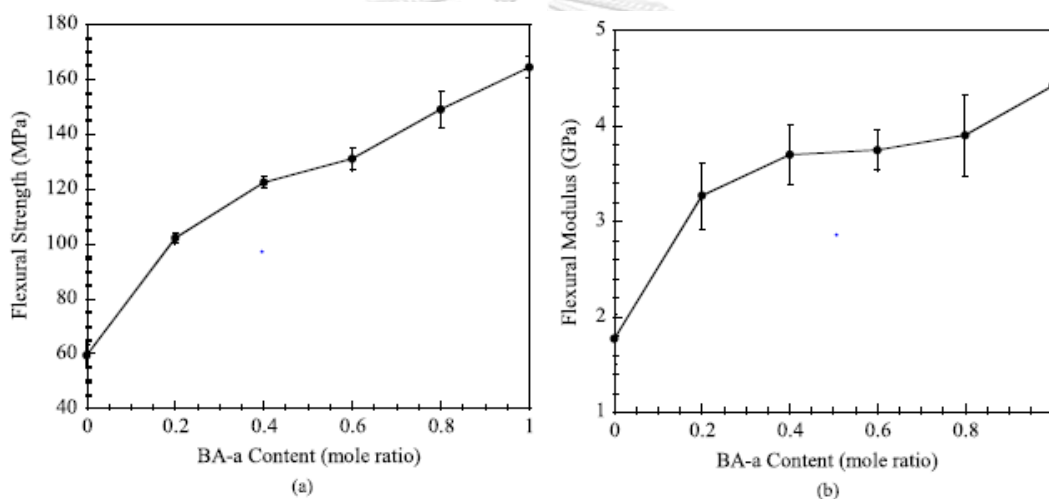


Figure 3.6 Flexural strength (a) and flexural modulus (b) of the benzoxazine-modified epoxy SMP samples at various compositions at room temperature [7].

The flexural strength values of the benzoxazine-modified epoxy SMPs were increased from 59.5 MPa for ENDB 1/1/1/0 to 164.3 MPa for ENDB 1/1/0/1. It can be observed that the flexural strength of the benzoxazine-modified epoxy SMPs increases with increasing BA-a content. The flexural modulus values of the benzoxazine-modified epoxy SMPs were increased from 1.8 GPa for ENDB 1/1/1/0 to 4.4 GPa for ENDB 1/1/0/1.

The addition of BA-a resin results in a systematic increase of the modulus of the obtained SMP. This could be due to the addition of the more rigid BA-a structure into the epoxy-based SMP increasing the stiffening of the resulting polymer alloys.

The shape recovery speeds of the benzoxazine-modified epoxy SMP are presented in Figure 3.7. All of the samples took only a few minutes to completely recover to their original shape, suggesting good shape recovery performance. At high temperature, the shape recovery time decreased because the movement of chain segments became intense, this caused an increase in the recovery force on the samples.

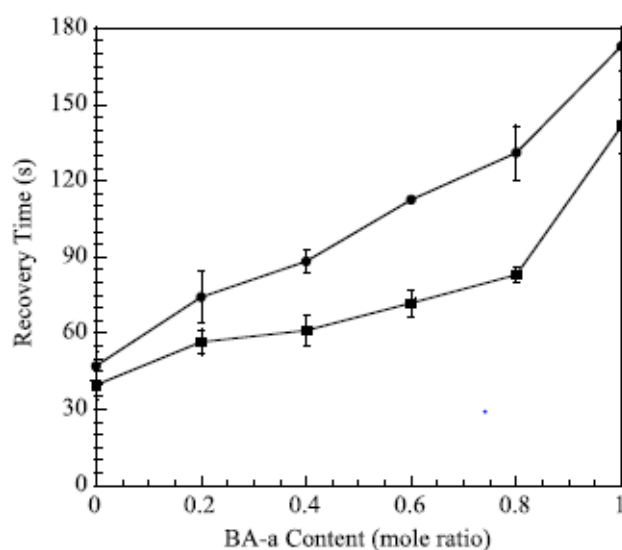


Figure 3.7 Recovery time as a function of BA-a content of the benzoxazine-modified epoxy SMP samples at various composition: (●) T_g , (■) $T_g+20^\circ\text{C}$ [7].

The recovery stress under flexural mode of the SMPs was measured from the transition stage of the shape-fixed stage to the recovery shape stage. The benzoxazine-modified epoxy SMPs samples with 0, 0.2, 0.4, 0.6, 0.8 and 1.0 mol ratio of BA-a showed recovery stresses of about 20.42 ± 0.39 , 23.36 ± 2.39 , 29.77 ± 0.87 , 30.97 ± 0.97 , 33.70 ± 3.01 and 38.18 ± 2.82 kPa, respectively, as seen in Figure 3.8. Based on

their results, the benzoxazine resin can substantially improve the recovery stress of epoxy-based SMPs due to the fact that the BA-a may be able to store elastic strain energy. When reheating the specimens, this stored elastic strain energy will release and the BA-a/epoxy-based SMPs thus render higher recovery stress

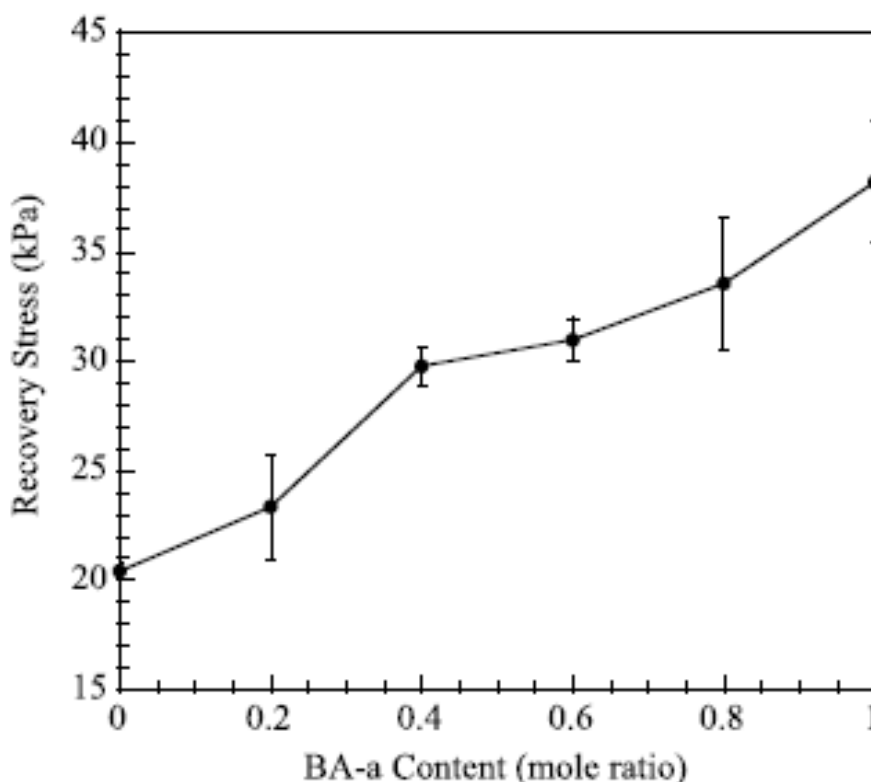


Figure 3 8 Recovery stress as a function of BA-a content of the benzoxazine-modified epoxy SMP samples at various compositions [7].

Sini et al. (2014) investigated the synthesis, polymerization mechanism, and thermal properties of vanillin-furfurylamine-based benzoxazine (V-fa). In the DSC scan (Fig. 3.9) of V-fa, a sharp melting endotherm was observed at 125 °C followed by a curing exotherm in the range of 179–232 °C with onset at 179 °C and a maximum at 205 °C. V-fa showed a low curing temperature perhaps due to the presence of ACHO group in the backbone structure. The formyl group has been reported to oxidize easily

to carboxylic group which catalyses the ring-opening polymerization of benzoxazine.

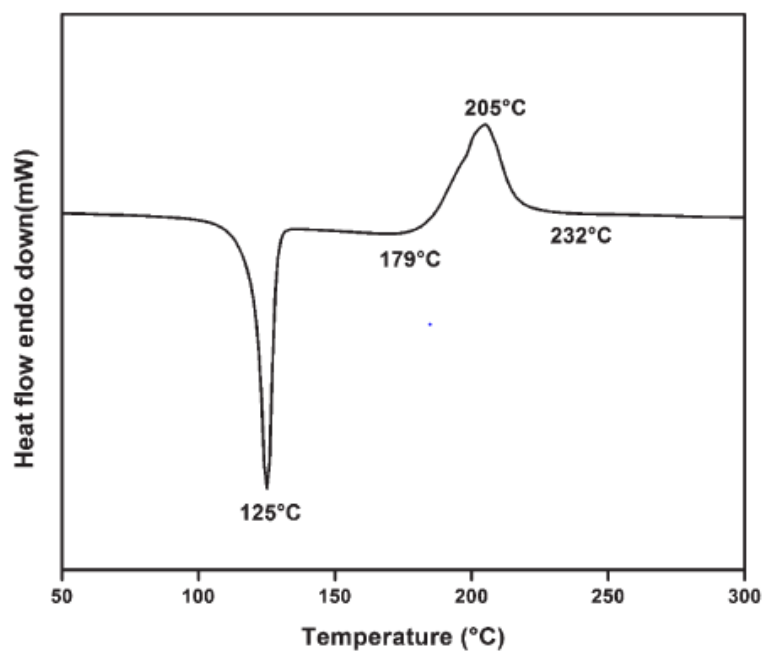


Figure 3.9 DSC trace of V-fa [17].

Thermal stability of V-fa was studied by TGA. The derivative mass loss curves of Va-Bz showed two-step degradation up to 250 °C (Fig. 3.10).

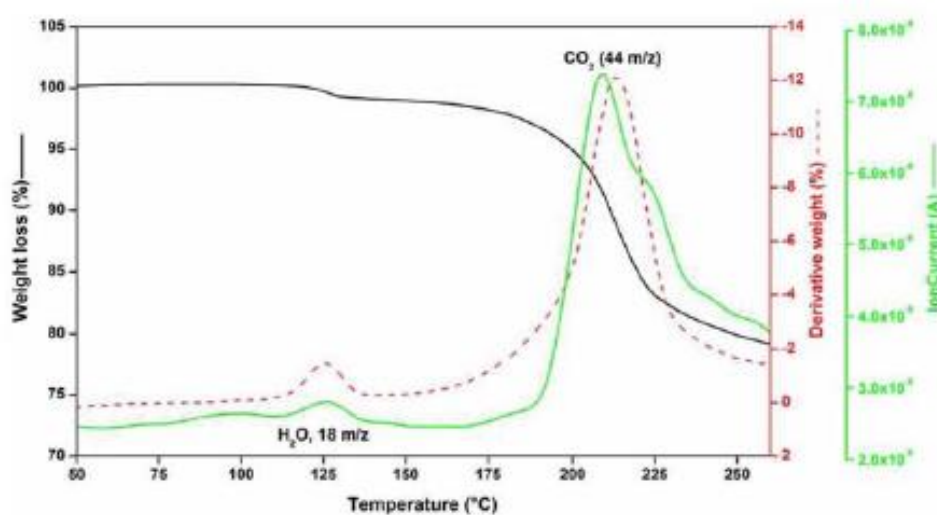


Figure 3.10 TG-MS trace of V-fa [17]

The first degradation step at 100 - 130 °C was accompanied by 2% mass loss which is assigned to moisture (H₂O) and the second degradation step at 179 - 240 °C was accompanied by 16% mass loss which is due to generation of CO₂ and other low molar mass products. The decomposition temperatures at 5% mass loss (T_{d5}) was 351 °C. The char yield at 800°C was 65%, which is attributed to the high cross-linking density. The glass transition temperature (T_g) for poly(V-fa) was 270°C, which can be considered as a measure of the rigidity of the polymer backbone.

Thirukumaran et al. (2014) studied synthesis two benzoxazine monomer from naturally occurring sources, i.e., eugenol (an extraction from clove), furfurylamine, stearylamine, and paraformaldehyde which a solvenless method was adopted to synthesize eugenol-furfurylamine-based benzoxazine monomer (F-Bz) and eugenol-stearylamine-based benzoxazine monomer (S-Bz). The structures of the benzoxazine monomers are supported by the FT-IR spectra as shown in Figure 3.11. The characteristic absorptions of the benzoxazine ring structure of both F-Bz and S-Bz appeared at 1233 and 1029 cm⁻¹, while the peak at 920 cm⁻¹ confirms the presence of a benzene ring with an oxazine ring attached to it which showed the existence of a reactive benzoxazine ring.

Moreover, the spectrum shows a peak at 1150 cm⁻¹ for both of the benzoxazines (F-Bz and S-Bz) due to the C–N–C symmetric stretching vibrations. The asymmetric and symmetric stretching vibration of methoxy carbonyl attached to the benzene ring was found at 1227 and 1011 cm⁻¹. Whereas both of the methylene groups (–CH₂), one in the benzoxazine ring and the other attached with the eugenol group, gave bands for its stretching vibrations between 2924 and 2854 cm⁻¹, respectively. The intensity of the C–H peaks (both symmetric and asymmetric) in S-Bz

is more when compared with F-Bz, indicating the presence of an alkyl side chain of stearylamine. The peaks observed at 1589, 995, and 733 cm^{-1} may be attributed to the vibrations of the furan ring.

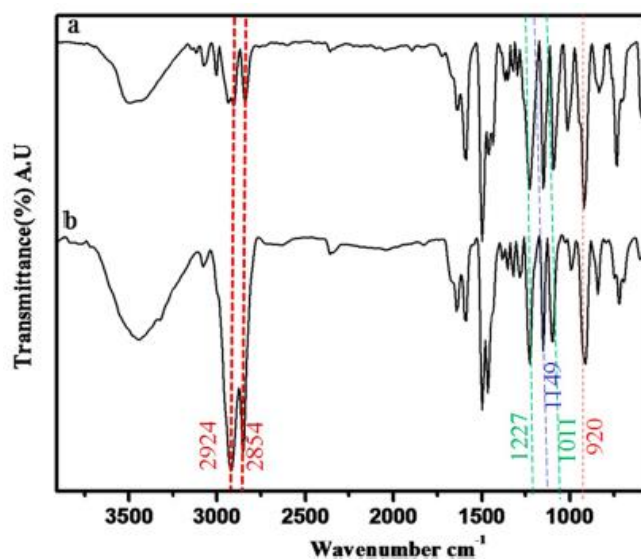


Figure 3.11 FT-IR spectra of (a) F-Bz and (b) S-Bz benzoxazine monomers [19].

The eugenol- furfurylamine- based polybenzoxazine (PF- Bz) , the eugenol- stearylamine- based polybenzoxazine (PS- Bz) and their copolymer were prepared by curing F- Bz and S- Bz mixtures which they were evaluated. As show in Table 3.3 The storage modulus, crosslink density and glass transition temperature (T_g) of PF- Bz were 3.33 GPa, 4.4 mol m^{-3} and 148 $^{\circ}\text{C}$, respectively which were higher than PS- Bz due to the rigid molecular stuture more than PS- Bz.

Table 3.3 Properties of PF-Bz, PS-Bz and their copolymer from DMA.

Sample	Molar Ratio of PS-Bz/ PF-Bz	Storage modulus, E' (GPa) at 30 °C	Crosslink density (mol m ⁻³)	T _g (°C)
a	100:0	2.82	3.7	101
b	75:25	2.94	4.0	106
c	50:50	3.12	4.1	125
d	25:75	3.29	4.4	154
e	0:100	3.33	4.4	148

Thermogravimetric analysis was used to study the thermal stability of the polymers and their copolymers. The thermogram is shown in Figure 3.12. The results indicated that PF-Bz shown the maximum thermal stability when compared with PS-Bz.

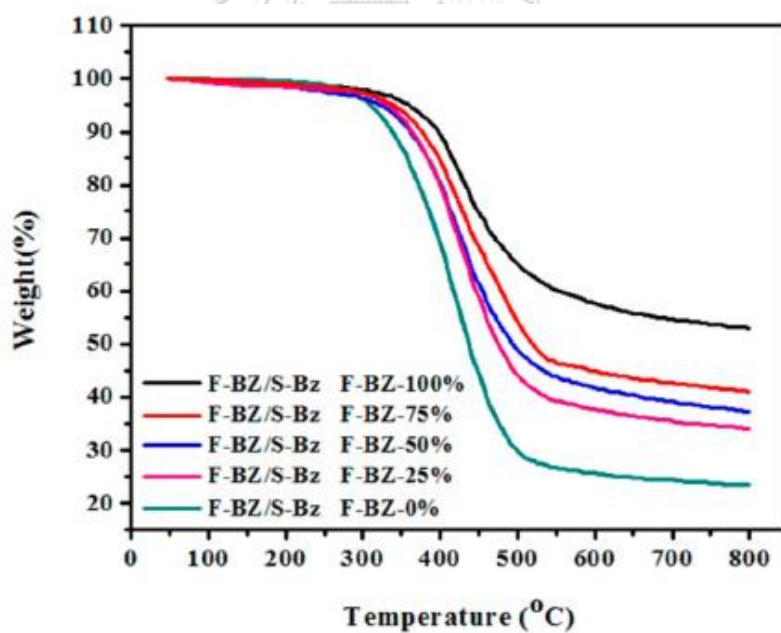


Figure 3.12 TGA curves of PF-Bz/PS-Bz mixtures with various F-Bz contents in molar ratios (a) 0%, (b) 25%, (c) 50%, (d) 75%, and (e) 100% [19].

Park et al. (2004) investigated the synthesis and thermal properties of epoxidized vegetable oils such as epoxidized soybean oil (ESO) and epoxidized castor oil (ECO). The cationic polymerization and thermal properties of ESO and ECO initiated by a cationic latent catalyst, N- benzylpyrazinium hexafluoroantimonate (BPH) . The polymerization of ESO and ECO was initiated at 80 and 50 °C, respectively. Figure 3.13 shows the conversion of the ESO/BPH and ECO/BPH which ECO is performed at a lower polymerization temperature than that of ESO due to their different structures. The reactive epoxide number per molecule of ESO (4.6) is higher than that of ECO (2.8). The steric hindrance induced by intra and intermolecular interactions in ESO is larger than that of ECO, resulting in a higher curing temperature in the cationic polymerization.

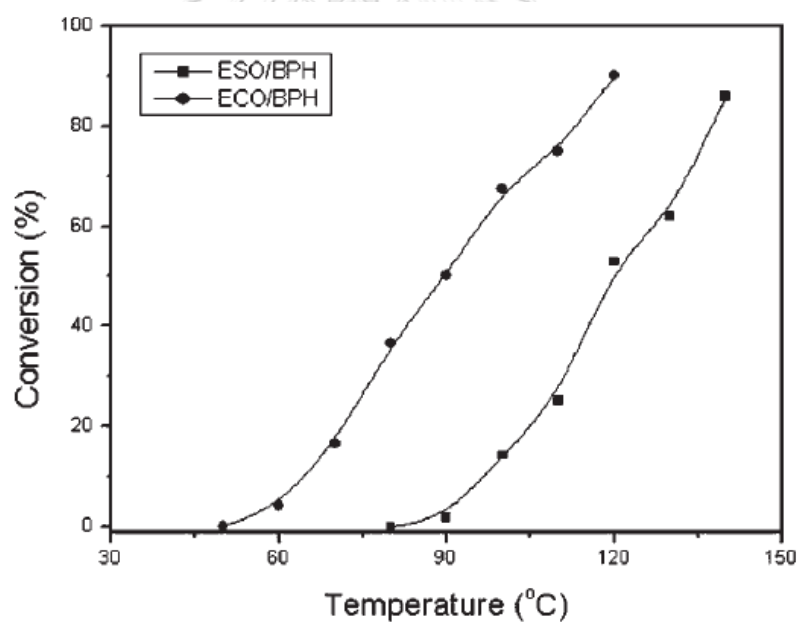


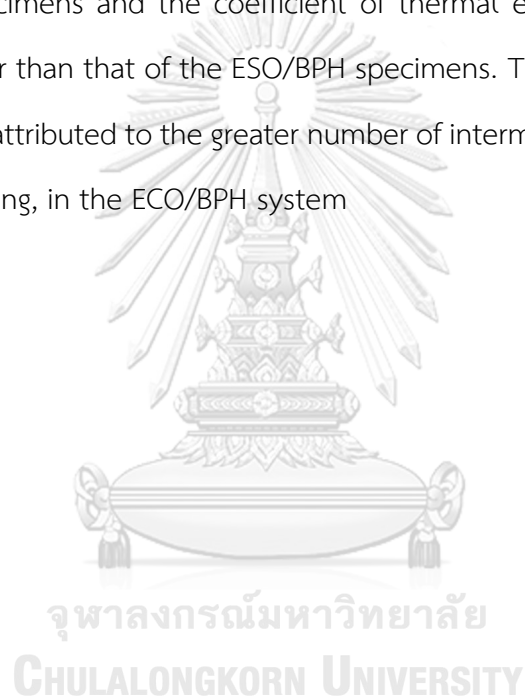
Figure 3.13 Relationships between ESO or ECO conversion and temperature in the polymerization with 1 wt.-% BPH for 2 h [10].

The glass-transition temperature and coefficient of thermal expansion of the ESO/BPH and ECO/BPH systems are listed in Table 3-4

Table 3.4 Thermal mechanical analysis of the cured ESO/BPH and ECO/BPH systems.

System	T _g (°C)	Coefficient of thermal expansion (10 ⁻⁵ /°C)	
		Glassy region	Rubbery region
ESO/BPH	24	12.8	21.2
ECO/BPH	38	10.8	20.5

The results indicate that the T_g value of the ECO/BPH specimens is higher than that of the ESO/BPH specimens and the coefficient of thermal expansion of the ECO/BPH specimens is lower than that of the ESO/BPH specimens. The authors concluded that this result can be attributed to the greater number of intermolecular interactions, such as hydrogen bonding, in the ECO/BPH system



CHAPTER IV

EXPERIMENTAL

4.1 Raw Materials

Materials used in this research are benzoxazine resin and aliphatic epoxy. Benzoxazine resin are vanillin-based benzoxazine and eugenol-based benzoxazine which based on vanillin, eugenol, furfurylamine and formaldehyde. Vanillin, Eugenol, and furfurylamine were purchased from Sigma-Aldrich Pte. Ltd. Paraformaldehyde (AR grade) was purchased from Merck Company. Aliphatic epoxy is epoxidized castor oil (ECO) was supported by Aditya Birla Chemical (Thailand).

4.2 Resin Preparation

4.2.1 Benzoxazine Resin Preparation

Vanillin-based benzoxazine resin (V-fa) was synthesized from vanillin, furfurylamine and formaldehyde at a mole ratio of 1:1:2. The mixture was heated to 105°C in an aluminum pan and was mixed until a homogeneous mixture was obtained for 1 h to yield a transparent yellow color monomer product, according to the patented solventless method.

Eugenol-based benzoxazine resin (E-fa) was synthesized from eugenol, furfurylamine and formaldehyde at a mole ratio of 1:1:2. The mixture was heated to 100°C in an aluminum pan and was mixed until a homogeneous mixture was obtained for 1 h to yield a pale yellow color monomer product, according to the patented solventless method.

4.2.2 Preparation of Benzoxazine-Epoxy Copolymer Specimens

The V-fa monomer was mixed with ECO. The weight percentage of the ECO was in the range of 10–50wt%. The mixture was heated to a temperature of 90°C in a

aluminum pan and stirred until a homogeneous mixture was obtained. The molten resin mixture was coated on glass substrates by a 300- μm thick doctor blades and thermally cured in an oven at 140°C/1h, 150°C/1h, 160°C/1h, 170°C/2h and 180°C/2h. After cooling down to room temperature, the cured poly(V-fa)/ECO copolymers were removed from glass substrates and taken to characterization.

The E-fa monomer was mixed with ECO. The weight percentage of the ECO was in the range of 10–50wt%. The mixture was heated to a temperature of 90°C in an aluminum pan and stirred until a homogeneous mixture was obtained. The molten resin mixture was coated on glass substrates by a 300- μm thick doctor blades and thermally cured in an oven at 160°C/1 h, 170°C/2 h, 180°C/2 h, and 190°C/2 h. After cooling down to room temperature, the cured poly(E-fa)/ ECO copolymers were removed from glass substrates and taken to characterization.

4.3 Characterization Methods

4.3.1 Thermogravimetric Analysis (TGA)

Thermal stability of bio-based benzoxazine/bio-based epoxy copolymer samples were performed on a thermogravimetric analyzer (model TGA1 Module) from Mettler-Toledo (Thailand). The testing temperature program was ramped at a heating rate of 20°C/min from 25 to 800°C under nitrogen atmosphere with a constant N₂ purge gas flow rate of 50 ml/min. The sample mass was approximately 5 to 10 mg. The degradation temperatures at 5% weight loss (T_{d5}) and char yields at 800°C of the samples were reported.

4.3.2 Dynamic Mechanical Analysis (DMA)

Thermomechanical properties of bio-based benzoxazine/ bio-based epoxy copolymer samples were obtained by a dynamic mechanical analyzer (DMA, model DMA242, Netzsch, Germany) which was used to obtain a storage modulus (E') and loss

modulus (E'') of the polymeric specimens. The sample had a dimension of 5 mm × 30 mm × 0.3 mm. The gauge length was approximately 10 mm for all samples. The samples were tested using a tensile mode at a heating rate of 5°C/min from -100°C to 200°C. A test frequency of 1 Hz and a strain amplitude of 5 μm under nitrogen atmosphere were employed.

4.3.3 Shape Fixity Test

Shape fixity of bio-based benzoxazine/bio-based epoxy copolymer samples were studied by a universal testing machine with a thermal chamber under a three point bending mode. Firstly, the first temporary shape was formed by applying force for 10% bending to a sample (10 mm × 50 mm × 0.3 mm) at $T_g + 20^\circ\text{C}$, then the sample was cooled to room temperature. The force was then removed completely to obtain a temporary shape (10% bending). The deflection after unloading was then measured, and shape fixity at each temporary shape of each sample was then determined.

The shape fixity (R_f) was calculated using Equations (4.1) according to a report by Xie [35].

$$R_f = \frac{\epsilon}{\epsilon_{\text{load}}} \times 100 \quad (4.1)$$

Where: ϵ_{load} = The maximum strain under load

ϵ = The fixed strain after cooling and load removal

4.3.4 Shape Recovery Performance

Shape recovery test of the sample upon bending load was performed as schematically outlined in Figure 1. The procedure for the thermo-mechanical bending cycle of the sample included the following steps. Firstly, the original shape of SMPs were kept in an oven at $T_g + 20^\circ\text{C}$. Then the sample was bent to a storage angle of in a 'U' shape. After that, the sample was kept at room temperature. The sample fixed

to the apparatus was put in an oven at $T_g + 20^\circ\text{C}$ and subsequently recovered to an angle θ_R . The shape recovery ratio (R_N) was calculated by equation (4.3), where r denotes the radius of the mandrel, t represents the thickness of the SMP specimen, θ_0 is the original storage angle of the specimen in the storage state during the first bending cycle. The value of the shape recovery ratio is calculated by

$$R_N = \left(1 - \frac{\theta_R}{\theta_0} \times 100\% \right) \quad (N = 1, 2, 3, \dots) \quad (4.3)$$

Where R_N denotes the shape recovery ratio of the N^{th} thermo-mechanical bending cycle, θ_0 is the original storage angle, θ_R is the angle of the tested sample at the recovery state. R_N are obtained through equations (4.3). In the following tests, the radius r of the mandrel and thickness t of SMP specimen are 2 mm and 0.3 mm, respectively.

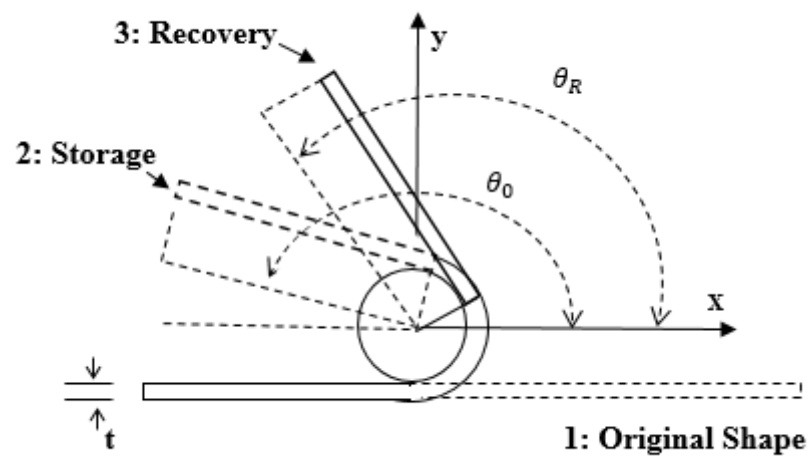


Figure 4.1 Schematic illustration of the setup for the shape recovery performance test

CHAPTER V

RESULTS AND DISCUSSION

5.1 Chemical structure of V-fa and E-fa based benzoxazine monomer

The IR spectra of V-fa and E-fa based benzoxazine monomer are shown in Figure 5.1. The BA-a based benzoxazine monomer (Figure 5.1a) were characterized by the band at 1228 cm^{-1} from the aromatic ether C-O-C stretching mode of an oxazine ring. The bands around 947 and 1497 cm^{-1} were attributed to the tri-substituted benzene ring[33].

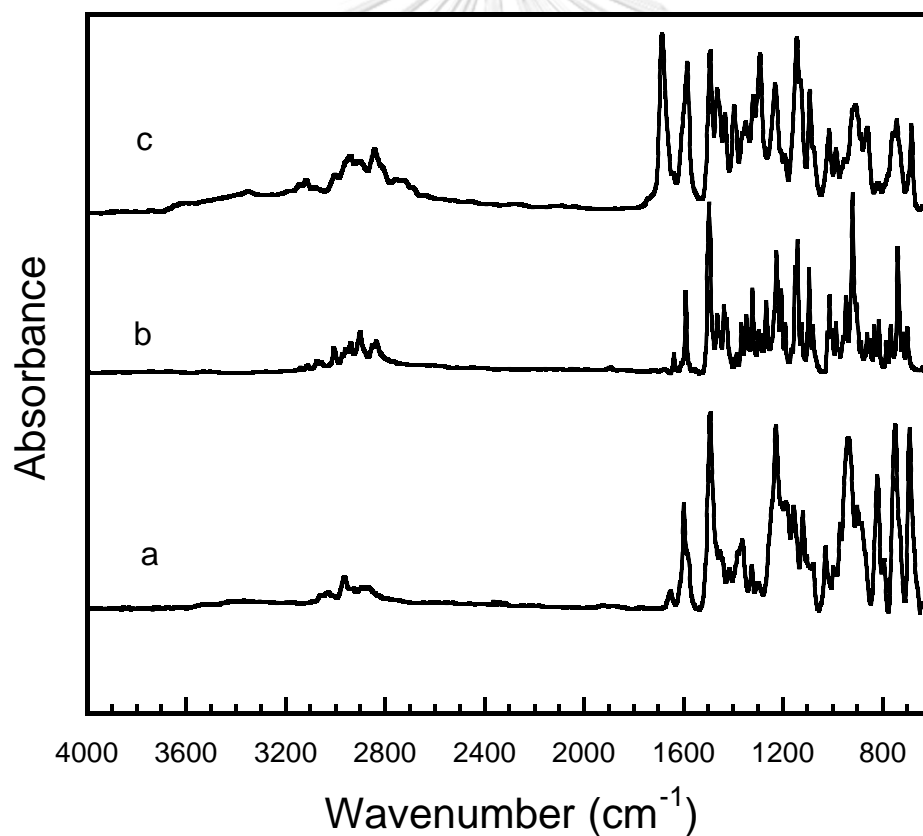


Figure 5. 1 FTIR spectra : (a) BA-a monomer. (b) E-fa monomer. (c) V-fa monomer

The E-fa based benzoxazine monomer (Figure 5.1b) displayed the peak at 1226 cm^{-1} from the aromatic ether C-O-C stretching mode of an oxazine ring. The peak at 919 cm^{-1} confirmed the presence of a benzene ring with an oxazine ring attached to it. The spectrum showed a peak at 1151 cm^{-1} from the C-N-C symmetric stretching vibrations. The peaks observed at 1001 and 738 cm^{-1} might be attributed to the vibrations of the furan ring[19].

The V-fa based benzoxazine monomer (Figure 5.1c) exhibits the absorption peaks at 907 and 1230 cm^{-1} of an oxazine ring. The furan group shown the peaks at 740 and 1586 cm^{-1} . The peak at 1686 cm^{-1} confirmed the presence of carbonyl groups of vanillin[17].

5.2. Thermal Stability of Bio-Based Benzoxazine/Bio-Based Epoxy Copolymer

Thermogravimetric analysis was employed to study the thermal stability of the samples. Thermal degradation temperature at 5wt% loss and residual weight at 800°C are important parameters used to determine the temperature stability of polymeric. TGA thermograms of the V-fa/ECO and E-fa/ECO copolymers are shown in Figure 5.2 and Figure 5.3, respectively. The samples were scanned from room temperature to 800°C with heating rate of 20°C/min under nitrogen atmosphere.

From Figure 5.2, the degradation temperatures (T_{d5}) of the neat poly(V-fa) and the neat ECO were 343°C and 351°C, respectively. T_{d5} values of the copolymer with ECO contents of 10wt%, 20wt%, 30wt%, 40wt% and 50wt% were 333, 323, 318, 317, and 314°C respectively. The results revealed that the thermal stability of V-fa/ ECO copolymer was decreased with increasing weight percentages of ECO. The char yield under a nitrogen atmosphere of the copolymer at 800°C decreased with increasing ECO contents. When the ECO contents were 10, 20, 30, 40, and 50wt%, the char yields of the copolymers were 62, 55, 48, 35, and 34%, respectively.

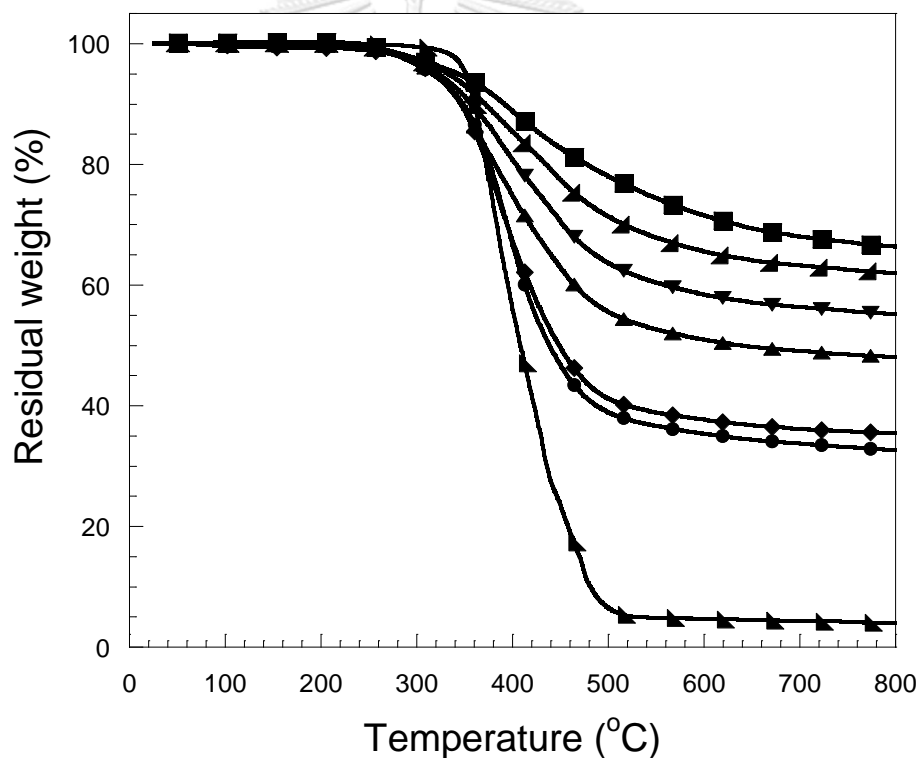


Figure 5.2 TGA thermograms of V-fa/ECO copolymers at various weight percentages of ECO: (■) neat poly(V-fa), (◄) 10wt%, (▼) 20wt%, (▲) 30wt%, (◆) 40wt%, (●) 50wt%, (►) neat ECO.

For thermal stability of the E-fa/ECO copolymers showed in Figure 5.3, the degradation temperatures (T_{d5}) of the neat poly(E-fa) and the neat ECO were determined to be 310°C and 351°C, respectively. The T_{d5} values of E-fa/ECO copolymers were 319, 320, 321, 323 and 328°C with ECO contents of 10wt%, 20wt%, 30wt%, 40wt%, and 50wt%, respectively. The T_{d5} values of copolymer were found to increase with increasing ECO content. The results indicated that the T_{d5} of the E-fa/ECO was found to be slightly higher than that of the neat poly(E-fa) which revealed that the thermal stability of polybenzoxazine network was improved upon the addition of ECO. In addition, the char yields of E-fa/ECO copolymer at 800°C was found to be 46, 39, 31, 25, and 23% at ECO contents of 10, 20, 30, 40, and 50wt%, respectively. The char yields of V-fa/ECO and E-fa/ECO copolymers decreased with increasing ECO contents.

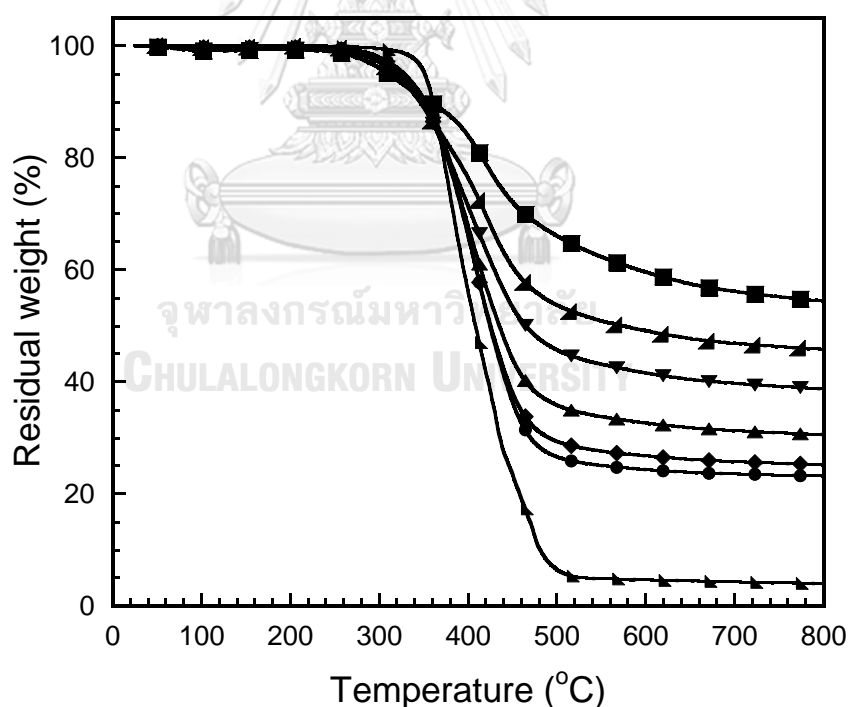


Figure 5.3 TGA thermograms of E-fa/ECO copolymers at various weight percentages of ECO: (■) neat poly(E-fa), (◄) 10wt% (▼) 20wt%, (▲) 30wt%, (◆) 40wt%, (●) 50wt%, (►) neat ECO.

5.3 Dynamic Mechanical Properties of Bio-Based Benzoxazine/Bio-Based Epoxy Copolymer

Dynamic mechanical properties of the V-fa/ECO and E-fa/ECO copolymers were exhibited in Figures 5.4 and 5.5, respectively. The viscoelastic properties of the samples were investigated by dynamic mechanical analyzer in a tensile mode. Several parameters such as storage modulus and loss modulus were obtained as a function of temperature in the range of -100°C to 200°C with a heating rate of $5^{\circ}\text{C}/\text{min}$. The storage modulus at the glassy state (-100°C) of V-fa/ECO copolymers having 20, 30, 40, and 50wt% of ECO contents were 2.27, 1.86, 1.73, and 1.59 GPa, respectively (Figure 5.4).

The storage modulus values of the E-fa/ECO at their glassy state (-100°C) were determined to be 1.53, 1.42, 1.21, and 1.16 GPa at ECO contents of 20, 30, 40, and 50wt%, respectively. The storage modulus of V-fa/ECO and E-fa/ECO copolymers tended to decrease with increasing contents of ECO. The reduction in the storage modulus values of the copolymer was due to the fact that ECO is an elastomer providing higher flexibility than V-fa and E-fa. This result suggested that the addition of ECO made the copolymer more flexible.

Glass transition temperature (T_g) of samples was determined from the peak maxima of loss modulus curves. The plots of the loss modulus as a function of temperature of the V-fa/ECO and E-fa/ECO copolymer samples were illustrated in Figures 5.6 and 5.7, respectively. In Figure 5.6, V-fa/ECO copolymers showed two loss modulus peaks or two T_g values, indicating the existence of two-phase structures. The T_g that was lower than 0°C was attributed to the ECO domain in the copolymer, while another peak at higher temperature was the T_g of V-fa/ECO copolymer. This result suggested that V-fa/ECO copolymers was a heterogeneous network composed of epoxy and benzoxazine domains. The ECO domain acted as the soft segment or the switch phase, while the V-fa domain acted as the hard segment or the stable phase.

The higher the phase separation, the better the shape fixity and shape recovery for shape memory polymer [25]. The T_g of V-fa/ECO copolymers with ECO contents of 20, 30, 40, and 50wt% were 158, 130, 110, and 100°C, respectively. In Figure 5.7, the T_g of the E-fa/ECO copolymers showed only one loss modulus peak or one T_g value, indicating the existence of one-phase structure. This result suggested that E-fa/ECO copolymer was a homogeneous network. The T_g of the E-fa/ECO copolymers were determined to be 40, 0, -12, and -17°C at ECO contents of 20, 30, 40, and 50wt%, respectively. These results indicated that the T_g of V-fa/ ECO and E-fa/ECO copolymers decreased with increasing in ECO contents. The reduction in T_g of the copolymers was attributed to the polymer chain flexibility of the ECO.

The shape memory performances of V-fa/ECO copolymer systems were better than those of E-fa/ECO copolymer systems due to the phase separation of the epoxy domain and the benzoxazine domain.

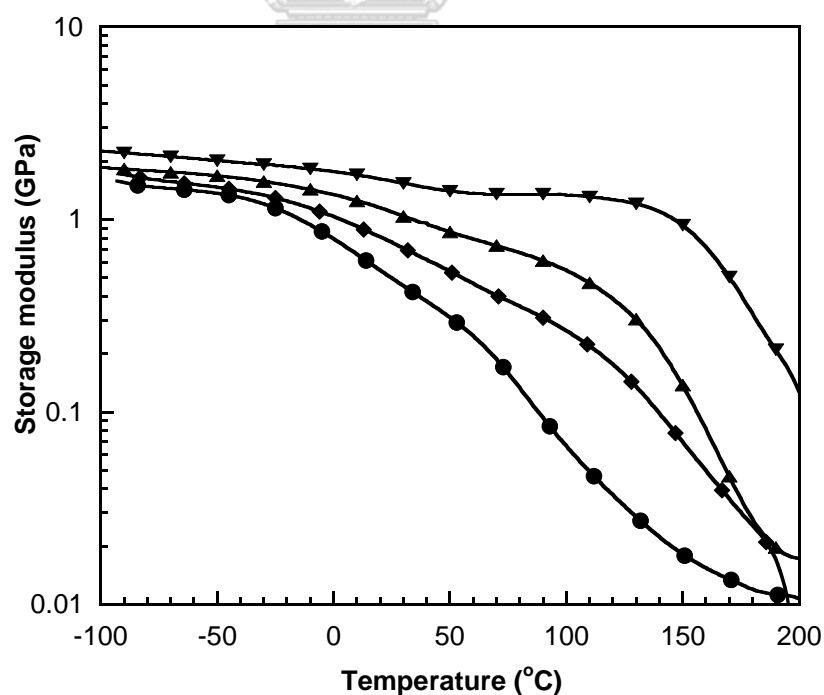


Figure 5.4 Storage modulus of V-fa/ECO copolymer at various weight percentages of ECO: (▼) 20wt%, (▲) 30wt%, (◆) 40wt%, (●) 50wt%

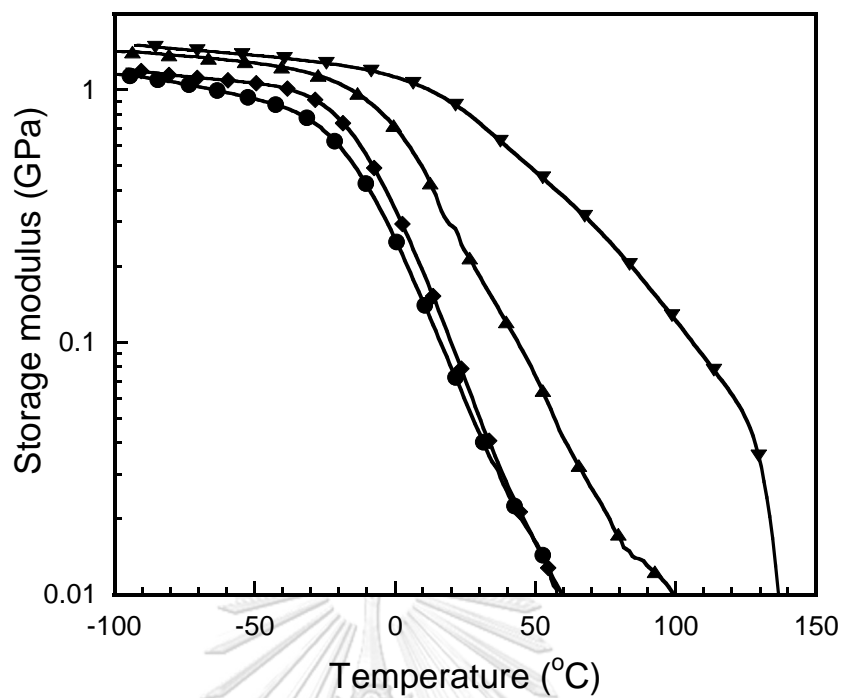


Figure 5.5 Storage modulus of E-fa/ECO copolymer at various weight percentages of ECO: (▼) 20wt%, (▲) 30wt%, (◆) 40wt%, (●) 50wt%

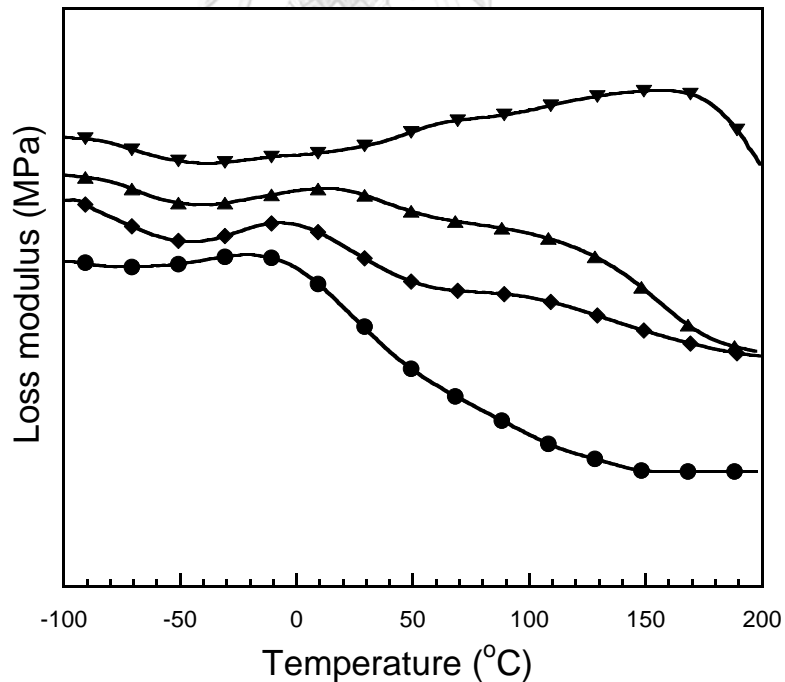


Figure 5.6 Loss modulus of V-fa/ECO copolymer at various weight percentages of ECO: (▼) 20wt%, (▲) 30wt%, (◆) 40wt%, (●) 50wt%

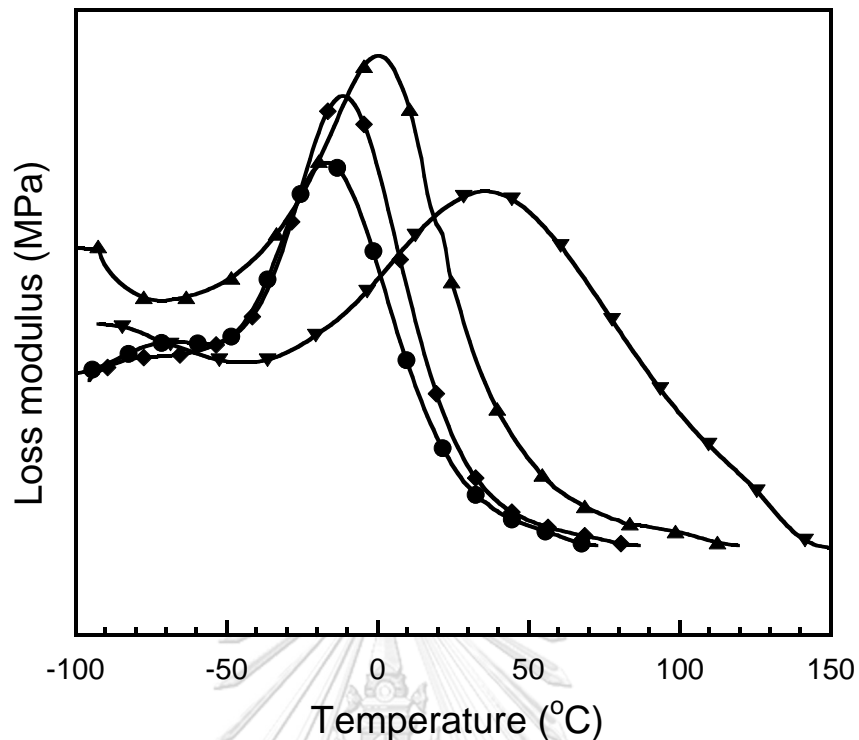
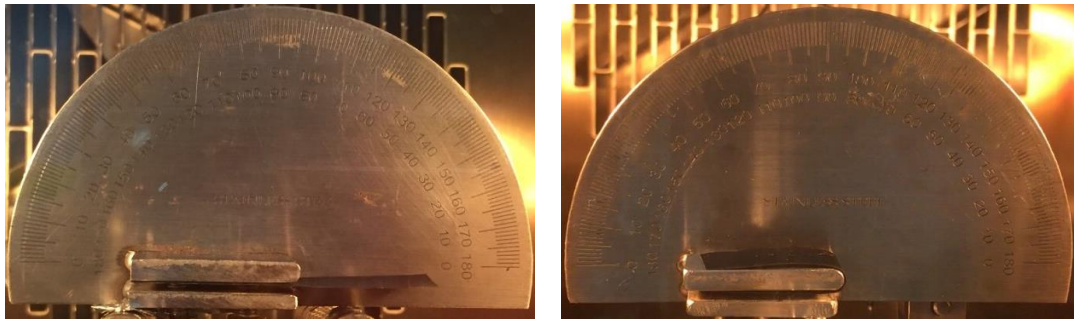


Figure 5.7 Loss modulus of E-fa/ECO copolymer at various weight percentages of ECO: (▼) 20wt%, (▲) 30wt%, (◆) 40wt%, (●) 50wt%

5.4 Shape Memory Properties

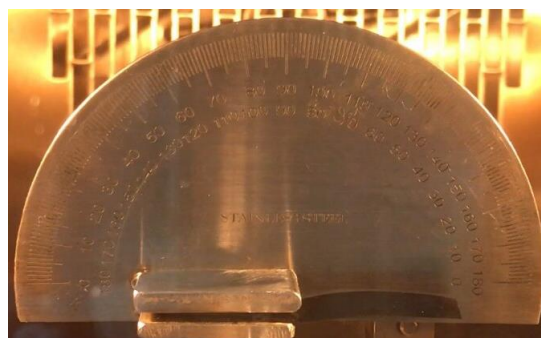
5.4.1 Shape Memory Behavior of Bio-Based Benzoxazine/ Bio-Based Epoxy Copolymer

The thermomechanical cycle tests used for investigating the shape memory of SMPs were carried out by a bending test at temperatures between room temperature and 20°C above T_g . The V-fa/ECO SMPs at 40wt% ECO content was used as the representative samples demonstrating the shape memory behavior as shown in Figure 5.8. The original rectangular shape (a) was heated at $T \geq T_g$ and deformed into a U shape through bending. Then, the deformed temporary shapes (b) were fixed by cooling under a load at room temperature. After re-heating above T_g , the sample was recovered into its original rectangular shape (c).



(a) Original shape

(b) Temporary shape



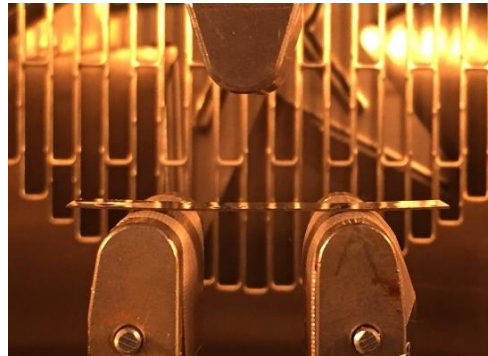
(c) Recovered shape

Figure 5.8 Shape memory behavior of V-fa/ECO SMPs at 40wt% castor oil based epoxy: (a) original shape, (b) temporary shape, and (c) recovered shapes

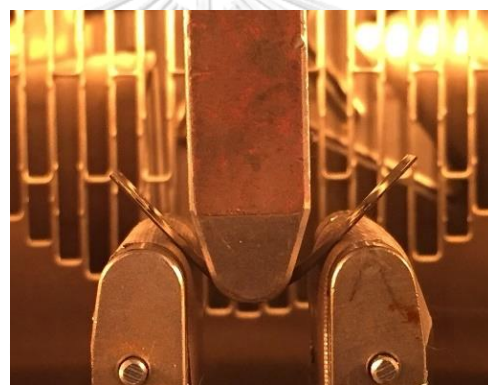
5.4.2 Effect of ECO Contents on Shape Fixity of V-fa/ECO and E-fa/ECO Shape Memory Polymer.

The shape fixity is an impotence parameter used to describe the ability of the SMPs to memorize the temporary shape or fixed shape. The shape fixity was investigated by a universal testing machine in a flexural mode (three-point bending mode). The various states of bending in SMPs are shown in Figure 5.9. The first stage at room temperature shows the original rectangular shape of V-fa/ECO SMPs (Figure 5.9a). The sample was heated to a temperature of $T_g + 20\text{oC}$ while deforming into the temporary shape by bending for 10% as exhibited in Figure 5.9b. Then, the sample

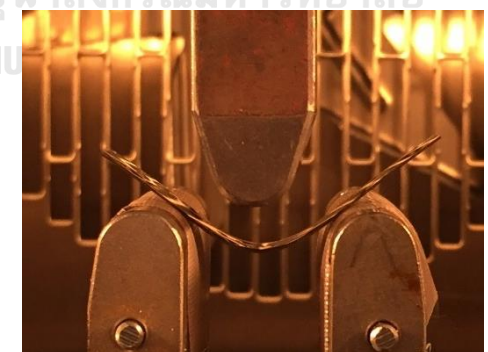
was cooled down to room temperature as shown in Figure 5.9c. In this step, the shape fixity was determined by equation 4.1.



(a)



(b)



(c)

Figure 5.9 Photographs showing various states of bending in shape fixity process for SMP samples: (a) first stage of samples, (b) deformed state of temporary shape at $T_g + 20^\circ\text{C}$ by bending for 10%, and (c) fixed state of temporary shape at room temperature

For E-fa/ECO shape memory polymer system, the SMP specimen could not be fixed at room temperature at the first stage which are shown in Figure 5.10. Therefore, the investigation of the shape memory properties was carried out only for V-fa/ECO shape memory polymer system.

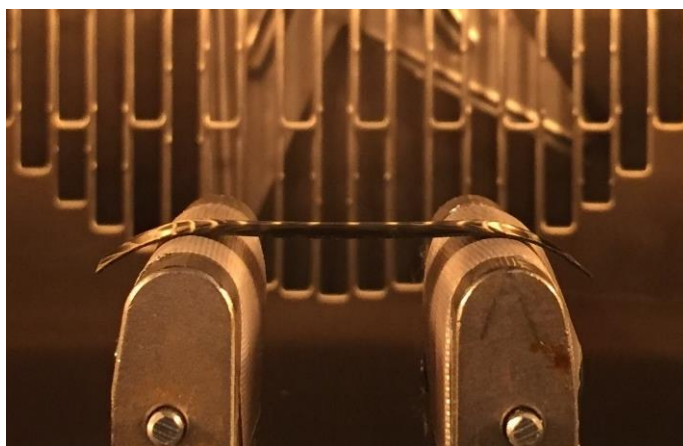


Figure 5.10 Photographs showing first stage of E-fa/ECO shape memory polymer system at room temperature.

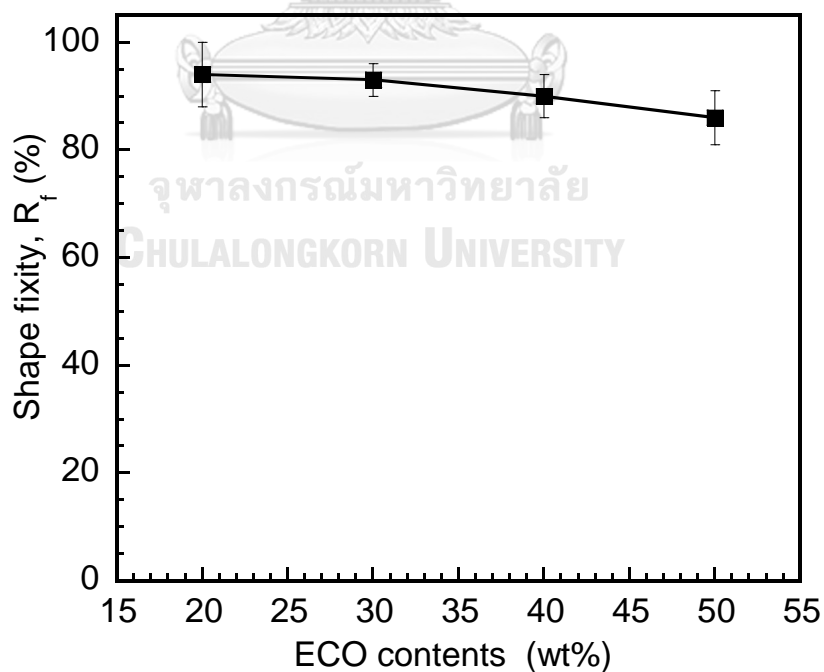


Figure 5.11 Shape fixity of V-fa/ECO at room temperature as a function of ECO contents at 20wt%, 30wt%, 40wt%, and 50wt%.

From Figure 5.11, the values of the shape fixity of V-fa/ECO SMPs were measured to be 94, 93, 90, 86 at ECO contents of 20wt% , 30wt% , 40wt% , and 50wt% , respectively. The shape fixity decreased with increasing ECO content. This behavior was due to the fact that SMPs consist of two segment, i.e. a stable network (hard segment) and a reversible switching transition (soft segment). The hard segment acts as the frozen phase, while the soft segment acts as the reversible phase. Moreover, a high glassy state modulus provided the materials with high shape fixity. A high glassy state modulus is an indication of high cohesive energy (mostly highly cross-linked polymer networks), leading to minimized propensity for creep related to shape change. Therefore, the decreasing of V-fa based benzoxazine which serves as the hard segment in the binary polymeric system with increasing ECO content resulted in a decreasing of shape fixity values.

5.4.3 Effect of ECO Contents on Shape Recovery of V-fa/ECO Shape Memory Polymer.

Shape recovery (R_N) is another parameter used to reflect how well an original shape of the sample has been memorized. The value of the shape recovery was determined according to Equation 4.4. In this study, the shape recovery process of the bent samples was recorded by a camera and their shape recovery angles were determined by measuring the angle between the straight ends of the specimens. The rectangular specimens were used to investigate the recovery process. As shown in Figure 5.12, the sample was heated up to the transition temperature ($T_g + 20^\circ\text{C}$) and held for 10 min. Then, the sample was bent into a U-shape of mandrel with a diameter of 4 mm. The fixed sample was cooled to room temperature and subsequently held for 10 minutes to ensure that the sample was firmly fixed in a U shape. In the next step, the bent sample was placed in an oven at $T_g + 20^\circ\text{C}$ for investigating the shape recovery performance.

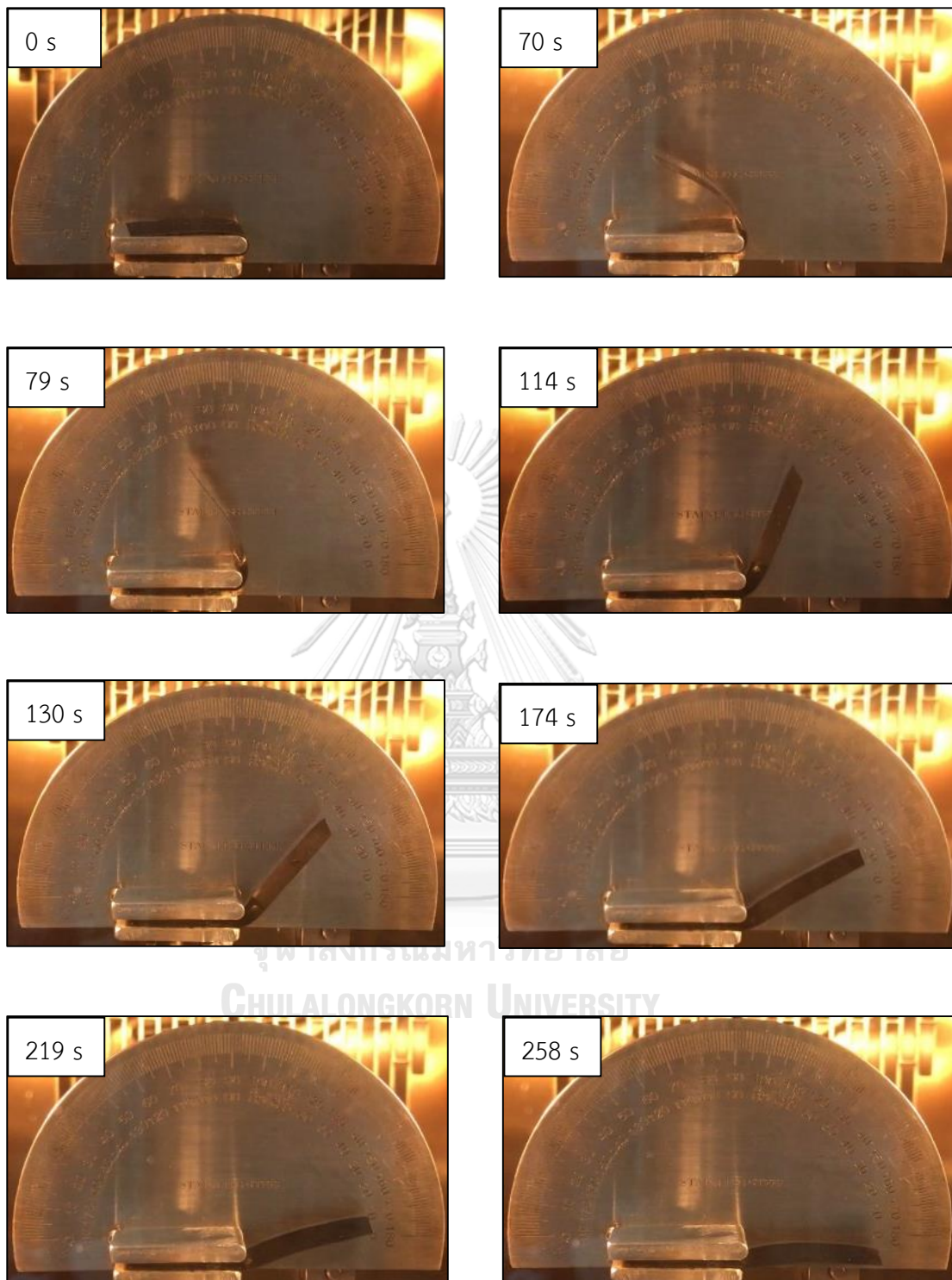


Figure 5.12 Series of images showed the shape recovery of the V-fa/ECO SMPs with 50wt% ECO content at $T_g+20^\circ\text{C}$.

Figure 5.13 illustrates a plot of shape recovery (R_N) as a function of ECO contents of the V-fa/ECO SMP samples. The values of the shape recovery of V-fa/ECO SMPs increased with an increase in the contents of the ECO. The shape recovery values of V-fa/ECO SMPs having 20, 30, 40, and 50wt% of ECO contents were 81, 87, 94 and 96, respectively. It was due to the fact that ECO has a higher chain flexibility than V-fa, affecting the deploying ability and recovery of the SMP samples. Therefore, increasing of ECO contents which serves as the soft segment in the binary polymeric system resulting in the enhancement of shape recovery performance.

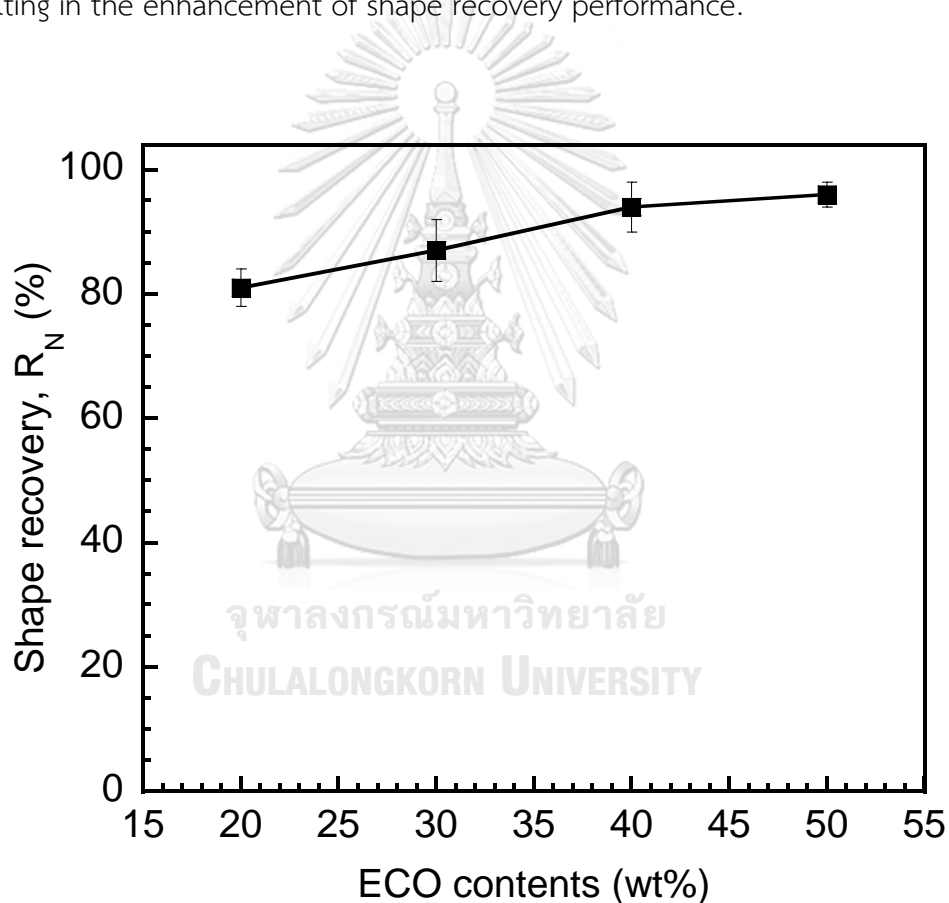


Figure 5. 13 Shape recovery of V-fa/ECO at $T_g+20^\circ\text{C}$ as a function of ECO contents at 20wt%, 30wt%, 40wt%, and 50wt%.

5.4.4 Effect of ECO Content on Shape Recovery Time

A plot of recovery angle as a function of recovery time for V-fa/ECO SMPs is shown in Figure 5.14. The slope of curve in Figure 5.14 remains constant from 50° to 150° at ECO contents of 40 and 50wt%. For below and above this range (50° to 150°), it was observed that V-fa/ECO SMPs had a relative low recovery rate at the start and the final stage. At the incipient stage, the release of constrained force was followed by a heavy friction among molecules, so that the slope was found to be low. After the incipient stage, friction force reduced under the gradual adjustment of segments. At terminal stage, shape recovery rate became slow once again because most of the constrained force has been released [36]. Shape recovery speed of the V-fa/ECO SMPs samples were evaluated at 10 minutes of shape recovery time. The results revealed that the recovery time of V-fa/ECO SMPs was increased with increasing weight percentages of ECO. The maximum recovery ratio for V-fa/ECO SMPs at ECO contents of 40 and 50wt% were reached within 10 minutes.

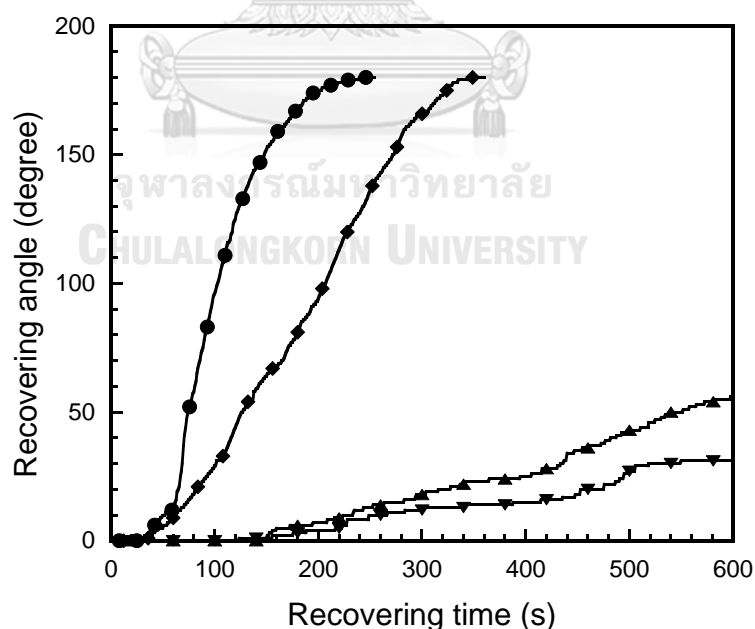


Figure 5.14 Recovery angle as a function of recovery time during the shape recovery process at $T_g+20^\circ\text{C}$ of the V-fa/ECO SMPs samples at various ECO contents : (▼) 20wt%, (▲) 30wt%, (◆) 40wt%, (●) 50wt%

5.5 Repeated fold-deploy cycles

Shape memorizing cycle indicates the performance in shape deforming applications. From our previous results, the V-fa/ECO SMP with ECO content at 40wt% provided SMP samples with good balance properties between shape memory performance and thermomechanical properties. Therefore, the specimen of V-fa/ECO SMP was subjected to a further investigation on shape fixing and shape recovering cycles.

From Figure 5.15, it can be seen that shape fixity values of V-fa/ECO SMP were not different up to 6 cycles, indicating that the shape fixity of the specimen was highly stable. However, the shape fixity value of V-fa/ECO SMP drastically changed after 6 cycles.

The shape recovery of the V-fa/ECO SMP specimen slightly increased within 5 cycles of the test (Figure 5.16). However, the shape recovery value of V-fa/ECO SMP abruptly decreased after 5 cycles of the tests.

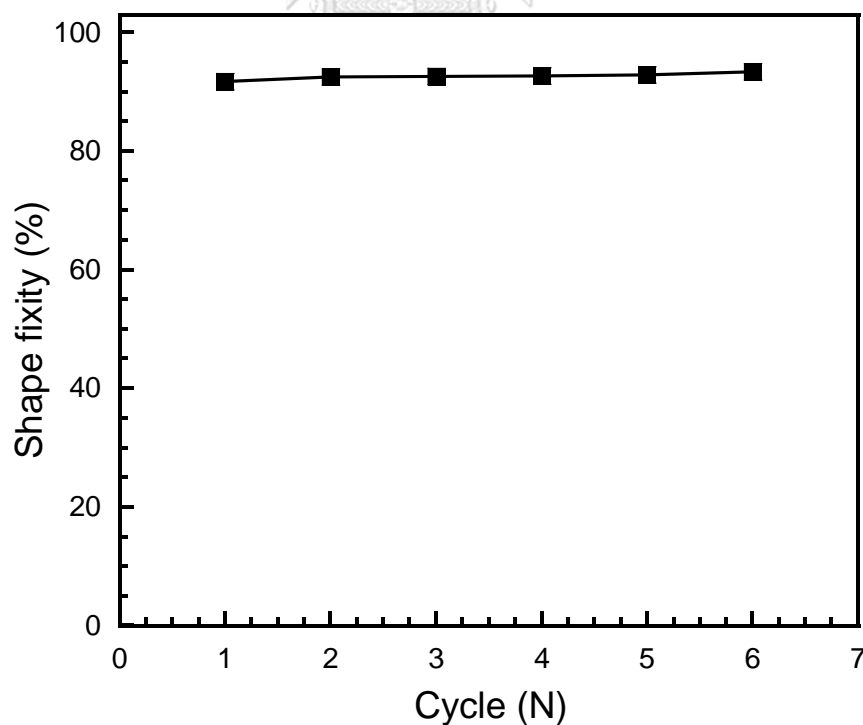


Figure 5.15 Shape fixity of V-fa/ECO at ECO content of 40wt% versus deformation cycle

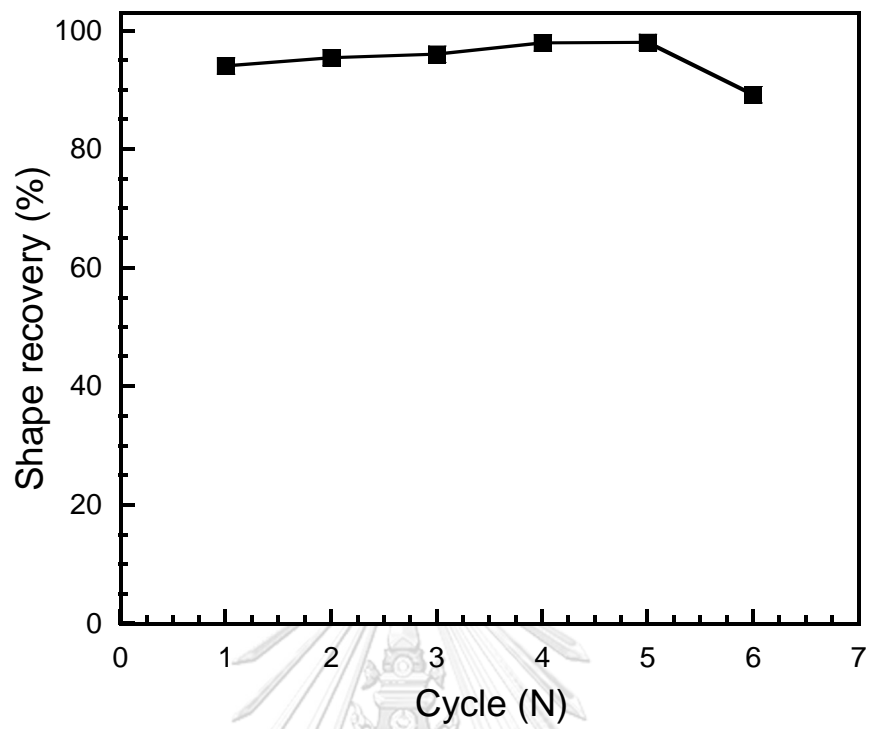


Figure 5.16 Shape recovery of V-fa/ECO at ECO content of 40wt% versus deformation cycle

CHAPTER VI

CONCLUSIONS

The binary system of benzoxazine/epoxy based shape memory polymer (SMP) was developed. Benzoxazine monomers (vanillin-based benzoxazine (V-fa) and eugenol-based benzoxazine (E-fa)) and epoxy (epoxidized castor oil (ECO)) were obtained from renewable resources. In this research, effects of ECO contents on thermal stability, mechanical properties, and shape memory performance of the developed SMP were evaluated.

The SMP films were successfully fabricated from V-fa/ECO and E-fa/ECO copolymer with ECO contents of 20, 30, 40, and 50wt%. Increasing ECO contents in V-fa/ECO and E-fa/ECO SMPs resulted in a decrease in storage modulus at their glassy state, enhancing the flexibility of the copolymer products. Glass transition temperatures of V-fa/ECO and E-fa/ECO SMPs decreased with increasing concentration of ECO. For thermal stabilities, the degradation temperatures at 5% weight loss (T_{d5}) of V-fa/ECO SMPs were found to decrease with increasing ECO contents, while the T_{d5} in E-fa/ECO SMP were found to increase.

The V-fa/ECO SMPs showed excellent shape fixity values at room temperature of 86–94%, while the temporary shape of E-fa/ECO SMPs cannot be fixed at room temperature. The V-fa/ECO SMPs provided shape recovery values of 81–96%. The shape recovery time of the V-fa/ECO SMPs increase with increasing ECO contents. The fastest recovery time (4 minutes) was obtained at the ECO content of 50wt%.

The V-fa/ECO SMP with ECO content at 40wt% provided the sample with good balance properties between shape memory performance and thermomechanical properties. Interestingly, the V-fa/ECO shape memory samples can be deformed up to 5 cycles.

The developed shape memory polymers based on renewable resources are attractive as a good candidate for shape memory materials showing promising potential in a wide range of applications.



REFERENCES

- [1] Behl, M., and Lendlein, A., Actively moving polymers. *Soft Matter*, 2007. 3: p. 58-67.
- [2] Meng, Q., and Hu, J., A review of shape memory polymer composites and blends. *Composites Part A: Applied Science and Manufacturing*, 2009. 40: p. 1661-1672.
- [3] Hager, M.D., Bode, S., Weber, C., and Schubert, U.S., Shape memory polymers: Past, present and future developments. *Progress in Polymer Science*, 2015. 49-50: p. 3-33.
- [4] Atli, B., Gandhi, F., and Karst, G., Thermomechanical Characterization of Shape Memory Polymers. *Journal of Intelligent Material Systems and Structures*, 2008. 20: p. 87-95.
- [5] Jin, F.-L., Li, X., and Park, S.-J., Synthesis and application of epoxy resins: A review. *Journal of Industrial and Engineering Chemistry*, 2015. 29: p. 1-11.
- [6] Santhosh Kumar, K.S., Biju, R., and Reghunadhan Nair, C.P., Progress in shape memory epoxy resins. *Reactive and Functional Polymers*, 2013. 73: p. 421-430.
- [7] Rimdusit, S., Lohwerathama, M., Hemvichian, K., Kasemsiri, P., and Dueramae, I., Shape memory polymers from benzoxazine-modified epoxy. *Smart Materials and Structures*, 2013. 22: p. 1-12.
- [8] Nouailhas, H., Aouf, C., Le Guerneve, C., Caillol, S., Boutevin, B., and Fulcrand, H., Synthesis and properties of biobased epoxy resins. part 1. Glycidylation of flavonoids by epichlorohydrin. *Journal of Polymer Science Part A: Polymer Chemistry*, 2011. 49: p. 2261-2270.
- [9] Stemmelen, M., Pessel, F., Lapinte, V., Caillol, S., Habas, J.P., and Robin, J.J., A fully biobased epoxy resin from vegetable oils: From the synthesis of the precursors by thiol-ene reaction to the study of the final material. *Journal of Polymer Science Part A: Polymer Chemistry*, 2011. 49: p. 2434-2444.

- [10] Park, S.-J., Jin, F.-L., and Lee, J.-R., Synthesis and Thermal Properties of Epoxidized Vegetable Oil. *Macromolecular Rapid Communications*, 2004. 25: p. 724-727.
- [11] Rimdusit, S., Jubsilp, C., and Tiptipakorn, S., *Alloys and Composites of Polybenzoxazines*. 2013: Springer.
- [12] Ishida, H., and Yee Low, H., A Study on the Volumetric Expansion of Benzoxazine Based Phenolic Resin. *Macromolecules*, 1997. 30: p. 1099-1106.
- [13] Wang, Y.-X., and Ishida, H., Development of low-viscosity benzoxazine resins and their polymers. *Journal of Applied Polymer Science*, 2002. 86: p. 2953-2966.
- [14] Tanpitaksit, T., Jubsilp, C., and Rimdusit, S., Effects of benzoxazine resin on property enhancement of shape memory epoxy: A dual function of benzoxazine resin as a curing agent and a stable network segment. *eXPRESS Polymer Letters*, 2015. 9(9): p. 824-837.
- [15] Li, S., and Yan, S., Synthesis and characterization of novel biobased benzoxazines from cardbisphenol and the properties of their polymers. *RSC Adv*, 2015. 5: p. 61808-61814.
- [16] Lochab B., Varma, I.K., and Bijwe, J., Thermal behaviour of cardanol-based benzoxazines. *Journal of Thermal Analysis and Calorimetry*, 2010. 102: p. 769-774.
- [17] Sini, N.K., Bijwe, J., and Varma, I.K., Renewable benzoxazine monomer from Vanillin: Synthesis, characterization, and studies on curing behavior. *Journal of Polymer Science Part A: Polymer Chemistry*, 2014. 52: p. 7-11.
- [18] Van, A., Chiou, K., and Ishida, H., Use of renewable resource vanillin for the preparation of benzoxazine resin and reactive monomeric surfactant containing oxazine ring. *Polymer*, 2014. 55: p. 1443-1451.
- [19] Thirukumar, P., Shakila Parveen, A., and Sarojadevi, M., Synthesis and Copolymerization of Fully Biobased Benzoxazines from Renewable Resources. *ACS Sustainable Chemistry & Engineering*, 2014. 2: p. 2790-2801.

- [20] Hayashi, S. , Tasaka, Y. , Hayashi, N. , and Akita, Y. , Development of Smart Polymer Materials and its Various Applications. Technical Review, 2004. 41(1): p. 1-3.
- [21] Zhao, Q. , Qi, H.J. , and Xie, T. , Recent progress in shape memory polymer: New behavior, enabling materials, and mechanistic understanding. Progress in Polymer Science, 2015. 49-50: p. 79-120.
- [22] Guo, J. , Wang, Z. , Tong, L. , Lv, H. , and Liang, W. , Shape memory and thermo-mechanical properties of shape memory polymer/carbon fiber composites. Composites Part A: Applied Science and Manufacturing, 2015. 76: p. 162-171.
- [23] Behl, M. , and Lendlein, A. , Shape-memory polymers. Materials Today, 2007. 10: p. 20- 28.
- [24] Meng, H. , and Li, G. , A review of stimuli-responsive shape memory polymer composites. Polymer, 2013. 54: p. 2199-2221.
- [25] Hu, J. , Characterization of shape memory properties in polymers, in Shape memory polymers and textiles. 2007, Woodhead Publishing Limited: England. p. 197-217.
- [26] Leng, J. , Lan, X. , Liu, Y. , and Du, S. , Shape-memory polymers and their composites: Stimulus methods and applications. Progress in Materials Science, 2011. 56: p. 1077-1135.
- [27] Rodriguez, E.D., Luo, X., and Mather, P.T., Linear/network poly(epsilon-caprolactone) blends exhibiting shape memory assisted self-healing (SMASH). ACS Applied Materials & Interfaces, 2011. 3: p. 152-161.
- [28] Petrie, E., Epoxy Adhesive Formulations. Hill, M: New York, 2006.
- [29] Paluvai, N. R. , Mohanty, S. , and Nayak, S. K. , Synthesis and Modifications of Epoxy Resins and Their Composites: A Review. Polymer-Plastics Technology and Engineering. 2014. 53: p. 1723-1758.
- [30] shida, H., Process for preparation of benzoxazine compounds in solventless systems, 1996, Edison Polymer Innovation Corporation: U.S.

- [31] Rimdusit. S, and Ishida. H., Gelation study of high processability and high reliability ternary systems based on benzoxazine, epoxy, and phenolic resins for an application as electronic packaging materials. *Rheologica Acta*, 2002. 41(1): p. 1-9.
- [32] Lligadas, G., Tüzün, A., Ronda, J., Galià, M., and Cádiz, V., Polybenzoxazines: new players in the bio-based polymer arena. *Polymer Chemistry*, 2014. 5: p. 6636–6644.
- [33] Ran, Q. , Gu, Y. , and Ishida, H. , Thermal Degradation Mechanism of Polybenzoxazines in Ishida. H, and Froimowicz. P (ed), *Advanced and Emerging Polybenzoxazine Science and Technology*. p. 171-204. Elsevier, 2017.
- [34] Ishida, H., and Allen, D.J., Mechanical characterization of copolymers based on benzoxazine and epoxy. *Polymer*, 1996. 37: p. 4487-4495.
- [35] Xie, T., Tunable polymer multi-shape memory effect. *Nature*, 2010. 464: p. 267-270.
- [36] Liu, Y., Han, C., Tan, H., and Du, X., Thermal, mechanical and shape memory properties of shape memory epoxy resin. *Materials Science and Engineering: A*, 2010. 527: p. 2510-2514.



APPENDIX

จุฬาลงกรณ์มหาวิทยาลัย
CHULALONGKORN UNIVERSITY

VITA

Ms. Phakakrong Hombunma was born in Kalasin, Thailand. She graduated at high school level in 2011 from Kamalasai School, Thailand. She received the Bachelor's Degree in Chemical Engineering from Faculty of Engineering, Khon Kaen University, Thailand in 2015. She continued his study for Master's Degree of Chemical Engineering at the Department of Chemical Engineering, Faculty of Engineering, Chulalongkorn University, Thailand. Some parts of this work were selected for oral presentation in the title of "Characterization of Novel Shape Memory Polymer from Green-Polybenzoxazine/Epoxy Alloy", during February 7-9, 2018 in The Pure and Applied Chemistry International Conference 2018 (PACCON 2018) at Hat Yai, Songkhla, Thailand





จุฬาลงกรณ์มหาวิทยาลัย
CHULALONGKORN UNIVERSITY